This document contains a point-by-point response to the reviews, including a list of all relevant changes made in the manuscript, and a marked-up manuscript version at the end of the document.

Reviewer 1

General comments
In this paper, the authors develop a statistical method for assessing CMIP5 climate model simulations of upwelling in the Senegalo-Mauritanian upwelling region and briefly discuss future projections of upwelling from a subset of the best-performing models. The method for assessing the models appears sound and seems to produce acceptable results in evaluating the models. However, I found the description of the method and its application difficult to follow at some points, as detailed in the specific comments below. There are also a number of typographical, grammatical, and organizational issues which impede the reader's ability to interpret the writing at some points.

I have provided some specific comments on some corrections needed in the technical corrections section, but this is not an exhaustive list and the authors should carefully proofread the paper prior to submitted any revised version. Finally, there seems to be a mismatch in the wind data discussed in the Data section versus the wind data used to produce Figure 10, as detailed in the specific comments below. All of these issues should be corrected before any subsequent version of the paper can be evaluated.

We would like to thank the reviewer for his/her careful reading of the manuscript and his/her relevant comments. We answered them carefully, and we believe the manuscript has definitely improved. We apologize for the typos and grammatical issues underlined by the reviewer. We have carefully revised the whole manuscript to improve this point specifically. We detail below ll the modifications that have been implemented in the text.

Specific comments
Lines 22-23: Give a brief summary of the main findings on the future behavior of the Senegalo-Mauritanian upwelling in the abstract, rather than simply stating that the future behavior was assessed.
This sentence was changed into "The future reduction of the Senegalo-Mauritanian upwelling proposed in recent studies is then revisited using this multi-model selection."

Lines 106-107: More detail is needed on the ERSST_v3b data set. How is this dataset produced, and why was it chosen as the "observation field" for comparison with the Models? Some details on the ERSST_v3b were added. We also explained that other data sets would have been available, in particular HadISST. A previous study has shown that differences in the Senegal-Mauritania upwelling are relatively weak. Yet, sensitivity of the method to the target field should definitely be addressed in the future, we thank the reviewer for this remark.

Lines 112-114: Similar to the ERSST_v3b data set, please provide some additional detail on the QUICKSCAT (sic) product. And is this product actually used in the paper?

In the caption for figure 10, the TropFlux data set is referenced rather than QuikSCAT in the discussion of the wind stress and Ekman transport (see comment on line 826), and there is no mention of QuickSCAT or TropFlux in the discussion of this figure in section 5.1. Additionally, "QuikSCAT" is the correct spelling of this satellite.
We apologize for the typo on the name of the satellite. We also apologize for the fact that QuickSCAT data is indeed not used in the final version of the paper. The wind stress was evaluated against the TropFlux reanalysis. Information about this product was added (end of section 2.1)

Line 118: Does "Sylla et al. (in rev.)" refer to the Sylla et al. 2019 Climate Dynamics paper, or another work? If this is another paper, it should be added to the reference List.
Sylla et al. (in rev.) and Sylla et al (2019) are indeed the same paper, accepted in the course of the preparation of the present manuscript. The citations have been homogenized, we apologize for this.

Section 3.2 (starting on line 168): It's not clear to me why the SOM classification followed by the HAC clustering was necessary. What is the reason for performing both classifications rather than just using one method or the other?

The SOM model has been used to determine a vector quantization of the dataset: i.e. to determine referent vectors that are a representative summary of the learning dataset. The vector quantization compresses the total database into a quite small (with respect to the size of the database) number of referent vectors such as each data is not too different of its nearest referent according to a distance (The Euclidean distance in the present case). The exact number of referents, that is the number of neurons, does not really matter because this number will be reduced by the HAC. Doing so allows us to take the non-linearities of the dataset into account in the analysis. The exact number at the end of the SOM+HAC procedure is not known a priori but at the end of the study by looking at the HAC dendrogram, which suggests several possibilities for the number of classes to estimate. A compromise between the number of classes we can explain from a physical point of view and the number we need to include the information embedded in the dataset is made. This procedure has been used with success in several papers (Jouini et al, 2016, JGR; Farikou et al, 2015, JGR; Sawadogo et al, 2009, IEEE; Niang et al, 2003, RSE).

We have added an introduction at the beginning of section 3 to explain this point. Note that it was also raised by reviewer 2. We are grateful to both reviewers for requiring this classification.

Lines 197-198: What is a "standard statistic algorithm"? Is this referring to the calculation of the standard deviation?
It refers indeed to the calculation of the spread in each neuron. We have re-phrased this sentence as:

"for each region-cluster, we estimated the monthly mean of the SST seasonal cycles and the associated spread captured by the neurons constituting this region-cluster" . Thank you for this clarification.

Section 3.4 (lines 255-330): Perhaps it is just my own ignorance, but I find figure 4 and the accompanying discussion quite difficult to interpret. What, conceptually, do the x and y axes and the grouping of the points on the plot represent? The description says that "proximity between a model and a region-cluster leads us to affirm that this region-cluster is well represented by that model", but the observations and the "highest skill" models 7 and 25 are far away from any of the region clusters. . .? And I think I understand that model 7 is considered as having good skill because it lies close to the "obs" point on the plot, but why is model 25 considered to have better skill than models 24, 19, 8, and 40, which are located a similar distance from the "obs" point as model 7? Have any previous studies used this method to assess the skill of models?

Sub-section 3.4 is now section 4. In fact the MCA method used in this section is different from the SOM and quite new in geophysics; it therefore deserves a dedicated section in which we give more details on the functioning of the MCA. We have rewritten the presentation of the MCA analysis in order to get an easier understanding of the functioning of this analysis and to facilitate the understanding of Figure 4. The new writing of the beginning of the MCA presentation (section 4) is shown below. Our changes are in yellow in this new writing.

"In order to further progress in the selection of the models, the 47 climate models and the Observation field were then analyzed by using a Multiple Correspondence Analysis (MCA in the following). MCA is a multivariate statistical technique that is conceptually similar to principal component analysis (PCA in the following), but applies to categorical rather than continuous data. Similarly as PCA, it provides a way of displaying a set of data in a two-dimensional graphical form.

In the following, we applied a MCA analysis to the (47 , 7) matrix $\mathbf{R}$ = [Rmi] whose elements represent the skills of the clusters of the models shown in front of the color bars in Fig. 3: the rows m represent the 47 different models, the columns i the 7 region-clusters. The MCA, as the PCA does, projects the initial matrix in a new basis in such a way that the new axes are the matrix eigenvectors (PC), the inertia of each axe being the related eigenvalues. According to the theory, the MCA matrix analysis gives 6=(7-1) independent PCs. Each model is now associated with a 6-dimensional vector. The MCA uses for this analysis the khi 2 distance. In figure 4, we present the projection of the models and the "region clusters" in the plane formed by the two first axes (x=PC1 and y= PC2) of the MCA that represent 70 % of the total inertia. Each model is represented by a small circle and each Region-cluster by a purple square. Moreover, we projected the observation field (green diamond) on that plane as a supplementary individual. The proximities in figure 4 is represented by the khi2 distance. To have a more precise view, it should be necessary to consider the projection on the 5 other PCs which represent 30% of the inertia.

In the (PC1, PC2) plane, the shorter the distance between two models, the more similar the distribution of their region-cluster skills. The seven clusters of the observation field are

represented by purple squares. Proximity between a model and a region-cluster leads us to affirm that this region-cluster is well represented by that model. ..;

……………

……………;

          In this above analysis, we must be aware that we are confronted to the intrinsic difficulty to represent multidimensional data in a plan. The representation of some data can be biased thank to the importance given to the other axes."

Line 826: What is the TropFlux data set? This needs to be described and its use justified in the Data section.
The TropFlux reanalysis combines the ERA-Interim reanalysis for turbulent and long-wave fluxes, and ISCCP (International Satellite Cloud Climatology Project) surface radiation data for shortwave fluxes. This wind stress product is described and evaluated in Praveen Kumar et al. (2011).
These lines were added in the Data section.

Technical corrections
The writing in this paper is frequently conversational in tone rather than technical, and there are many instances of imprecise filler words like "very", "pretty", and "nicely".
In line 250, "let us say. . ." is a conversational phrase that is not appropriate to use in a scientific manuscript in this context.
Also, the mention of "ongoing studies in our group" (line 527) is fine for a conference presentation but, in my opinion, is not appropriate to write in a scientific paper.
Please proofread the paper and correct these and other such instances of informal language.
The text was largely revised and improved in this respect. The two specific sentences cited above were corrected. We thank the reviewer for this remark that led us to significantly improve the language of the manuscript.

There are several excessively long paragraphs that are taxing on the reader. For example, the paragraph from lines 30-73 in the Introduction and the paragraph from lines 332-377 in section 4 are very difficult to read due to their length. Please break up and reorganize these and other long paragraphs.
These two paragraphs and several others have been cut. Thanks also for this remark that improves the readability of the paper.

There are a number of typographical and grammatical errors throughout the paper, which impede its interpretability to the reader in some places. I have given a few examples below, but this is not an exhaustive list, and the authors should check the entire paper carefully for such errors in any subsequent versions of the manuscript.

- Title: Extra space after the word "in"
Corrected

- I am not able to read the full "short summary" on the discussion paper web site, but the part I can see contains three misspelled words.
We are not sure why the short summary could not be read from the website, but the short summary was corrected

- Errors in capitalization of words (e.g. "Observation field" in line 108, seasonal "Cycle" in line 299)
These capitalizations intended to put emphasis on the elements of the mathematical procedure. Yet, we realize that this was not clear so that we removed all the capital letters in these expressions.

- Lines 16-18: Abrupt shift from first-person to third person ("We used a neural classifier. . ." to "One can then determine. . .")
corrected

- Line 83: Typo ("lies at is the southern. . .")
corrected

- Lines 109-110: Typo ("were been regridded")
corrected

- Line 525: Typo ("costal" instead of "coastal")
corrected

Line 16: Typically self-organizing maps are described as an "artificial neural network" rather than a "neural classifier".
This was changed: In the text we now use a artificial neural network (Self-Organizing Maps),

Line 21: What is meant by the phrase "performing multi-model ensemble"?
This phrase was changed to "an efficient multi-model combination of 12 climate models"

Line 26: CMIP5 stands for the "Coupled Model Intercomparison Project, Phase 5" (not the "5th Climate Model Intercomparison Project").
corrected

Line 383: Shouldn't this say "(Fig. 8, left)"?
Corrected, apologizes for this mistake

Line 755: Figure 1 appears distorted and blurry in the PDF version of the paper. Please correct this figure to make it easier to read.
This figure was corrected and the .eps version attached to the revisions is not blurred.

Reviewer 2

Mignot et al. use self organising maps to evaluate the behaviour of a multi-model ensemble in the Senegalo-Mauritanian upwelling region, with the aim of producing accurate projections of future climate changes in the region. Their algorithm aims to select models that yield a specific desired quantity - in this case, a multi model mean. They then project the selected models through the future to assess changes in the region.

There is clearly a great deal of potential in the technical work in this paper. The idea of using Self Organising Maps as a dimension reduction and interpretation technique is a good one, and appears to work very well. It can clearly add a great deal of value to the analysis of a large multi-model ensemble in this region. However, I feel a degree of restructuring, clarification of the aims of the paper, and editing for overall clarity is required before the scientific content can be properly assessed.

We would like to thank the reviewer for his/her careful reading of the manuscript and his/her constructive and challenging comments. We have restructured the manuscript as suggested, and clarified the methodology as much as we could. This has greatly improved the manuscript. We have also paid specific attention to editing issues for which we apologize. We detail below on all the modifications that have been implemented the text.

I feel the paper would most benefit from restructuring so that the objectives, details and then method of assessment of the algorithm were more clearly laid out earlier in the paper, and the reader were more carefully led through that process. As it stands, intense technical detail follows very broad overview statements, and important details about the analysis are left until later in the paper, so the reader is left confused and searching for appropriate context into which to place technical detail. Some choices in the analysis feel arbitrary, and it is unclear whether this is because they are indeed arbitrary, or that they are inadequately described.

The most obvious candidate for restructuring is the start of section 3, describing the methods used for classification of the models. This section dives straight into a detailed description of self organising maps (SOMs), without a discussion of precisely what the algorithm aims to achieve, how that can be assessed, and why SOMs were chosen as opposed to any other dimension reduction technique. As it is, the paper reads as "we decided to use SOMS and this is what you can do with them", rather than "we are trying to solve a specific problem and here is how SOMs can help". One suggestion would be to take the description of the methods from the start of section 6 (Discussion and Conclusion), expand upon it and place it at the start of section 3.

The SOMs appear to successfully cluster the model field into regions with different dynamics. This seems useful and interesting. How does it help solve the specific problem? I think it would be useful to set out near the beginning of the paper the exact strategy that will be used, and how to tell if it is successful or not.

Thank you for these detailed and constructive remarks. We restructured the paper by taking the remarks of the reviewer exposed in the above paragraphs into account. First, at the end of the introduction we now mention that our method is based on classification. At the beginning of section 3, we now justify the use of a classification method on the one hand and then choice of the SOM+HAC on the other hand.
Moreover, Sub-section 3.4 is now section 4. In fact the MCA method used in this section is different from the SOM and quite new in geophysics; it therefore deserves a dedicated section in which we give more details on the functioning of the MCA.
We also cut some long paragraphs in smaller paragraphs in order to facilitate the understanding of the text.

Regarding the relevance of the SOM in particular, note that this question was also raised by reviewer 1. We are grateful to both reviewers for requiring this classification. As answered above, the SOM model has been used to determine a vector quantization of the dataset: i.e. to determine referent vectors that are a representative summary of the learning dataset. The vector quantization compresses the total database into a quite small (with respect to the size of the database) number of referent vectors such as each data is not too different of its nearest referent according to a distance (The Euclidean distance in the present case). The exact number of referents, that is the number of neurons, does not really matter because this number will be reduced by the HAC. Doing so allows us to take the non-linearities of the dataset into account in the analysis. This explanation now appears at the beginning of section 3.

For example, It seems clear that the assessment algorithm (starting line 232) can be used to rank the models in terms of their closeness to observations and dynamics in particular regions.

One downside however, is that it does not give the modeller an intuition into how far the model is from "good" behaviour in absolute terms. We simply get an averaged "skill score" from 28% to 79%, but without an idea of how this might relate to more traditional measures of skill. So how close is the best model and how far is the worst model from reality? We have only a score (useful as that is) to guide us.

In this paper we give a global index that is the mean of 7 indices associated with the seven Region-clusters. This mean index shows the ability of a given model to represent the global area. But for each Model and each Region-Cluster, we give the ratio that represents how that model represents that Region-cluster. These indices are visible on the colorbar of figure 3.So each modelling group can evaluate how its numerical schemes represent the dynamic of the observations.
We also give a visual interpretation of the fitting of the different CMIP5 models with respect to observations in Figure 4. The best models are the closest to the observations with respect to the khi2 distance.
In general, we agree with the reviewer that there is a huge amount of information to take out from this method in general and from Fig. 3 and 4 in particular. Each modelling group could use this information to better understand the reasons for their model's difference to observation. And specialists of the Senegal-Mauritania region can use it to better understand the reasons for the

weak representation of this region in climate models. In this paper we propose an illustration of the method application. After publication, the method will be free of use for more various applications. We thus added a sentence in the text as well as in the conclusion to stress that point. We are grateful to the reviewer for having stressed that point.

The paper makes the claim that it offers an objective method for the assessment of the behaviour of models with regards historical observations. I struggle to accept this, given the number of subjective choices made with regards to the way the analysis is conducted. Subjective judgements will always need to be made in the analysis of climate model output - this is inevitable, and perfectly reasonable as long as labelled as such. The paper only examines a subset of model fields for example, and a subjective choice as to which of those fields to select has been made.

The reviewer is right in several aspects:

- The study focuses on the ability of CMIP5 models to reproduce the ocean seasonal variability in the Senegalo-Mauritanian upwelling region only. The models which represent this region at best do not necessarily represent other regions at best. Our study is not devoted to the comparison of the CMIP5 models in general but to their ability to reproduce the Senegal-Mauritanian upwelling area only. We now mention that point explicitly in the conclusion. Furthermore, a full representation of the geophysical phenomenon should involve more variables, as explained in Sylla et al (2019) and this first study is more a test-case than a full analysis.

- Concerning the use of statistics, we are aware that statistics are only a support to understand or interpret what is hidden in the dataset, mainly if the number of data and observations is large. This is the present case because we want to compare 47 different models with respect to a set of observations, with a focus on the dynamical behavior of each dataset (multidimensional analysis in a 12-dimensional space, the monthly SST anomalies). We built a method to solve that problem. Other methods could possibly lead to different results depending of what we looked for: The number of possible statistical studies is huge. In that sense, the choice of the method contains some subjectivity.

Nevertheless, the method we propose is not subjective ; it allows to rank the models according to the reduction of information we made (the seven dynamical region-clusters, after the SOM). This is in some way a classical problem in geophysics, where we need to classify, organize the information. Here it is done using relatively novel statistical tools (SOM+HAC). Finally, the MCA is a qualitative (but rational) method to summarize and visualize on a graphic the "similarities" of the models, the observations and the region-clusters.

For these reasons, we consider that the title is not misleading: our method is a step *towards* an objective assessment. Yet, considering the reviewer's remark, we have modified the sentence claiming for an "objective method" in the abstract and this term is now better justified in the conclusion section.

A core problem that needs to be addressed in the paper can be illustrated by considering the section starting on line 285:

"As indicated in the introduction, the main objective of the methodology is to select an ensemble of models that represents at best the upwelling behavior with respect to the observations and to use this ensemble to predict the impact of climate change in the Senegalo-Mauritanian upwelling with some confidence. The problem is now to determine a subset of models that can adequately represent the observations, as the number of models is small enough we choose to cluster them by HAC according to their projections onto the seven axes provided by the MCA, and select the optimal jump in the hierarchical tree (Jain and Dubes, 1998)."

I cannot see a description of what it means for a subset of models to "adequately represent the observations".

We agree with the reviewer that the phrase "adequately represent the observations" is misleading.
Through MAC+HAC, we group the models into Model-clusters, using the khi2 distance, according to their proximity to the observations and their internal similarity. Model group 4 appears as the one closest to observations with respect to that distance. In Figure 4, we see the projection of the individual models on the first two axes of the MCA. The fact that only two axes are shown here can introduce some bias in the visualization and this figure must be considered with some caution. We associated a multi-model with the Model-group 4 (close to the observations),whose outputs are the mean of the outputs of the models constituting the Model-group 4. We agree with the fact that we cannot prove that this is the best. An exhaustive research in order to find the best subset is nevertheless prohibitive due to the enormous number of possible combinations. The phrase "a subset of models that can adequately represent the observations" was changed into "a subset of models which has a better skill than Model-All".

I also cannot see an adequate description for what the "optimal jump in the hierarchical tree" of Jain and Dubes (1998) is, or what it might mean for the ensemble members. The clustering of the models in figure 4 looks reasonable by eye, but there are a large number of other ways that the models could be clustered that might be equally as reasonable. The authors claim that their algorithm selects a number of ensemble members that best represent an ensemble mean. I don't believe that they provide sufficient justification for why the ensemble mean should be selected for, or that the ensemble members their algorithm selects members in a way that is superior to a subjective selection.

We recall that the HAC (hierarchical ascending clustering) is a bottom-up algorithm for dataset clustering. The key operation in hierarchical bottom-up clustering is to repeatedly combine the two nearest (according to a certain distance) clusters into a larger cluster. The HAC starts from individuals and combines them according to their similarity (with respect to the chosen distance) to obtain new clusters.The process is repeated up to get one cluster only (the full dataset). This algorithm is visualised by a tree-like diagram, the so-called connection tree : the

connections between the clusters are represented by the branches of the connection tree (see figure below) according to their proximities. Due to the bottom-up algorithm, the construction of clusters is therefore objective with respect to the chosen distance. The objects are finally categorized into a hierarchy similar to a tree-like diagram which is called a dendrogram (see figure). A major problem then arises: When do I stop combining clusters and consider that I have optimal clusters?

The problem is semi-qualitative. It depends on the dataset under study. Most of the time, it is a compromise between a sufficient number of clusters to explain the complexity of the dataset and a relatively small number of clusters in such a way that every cluster can be handled and explained.

In the present study, we decided to deepen the statistical aspect of the problem and to choose an "optimal" model according to the data provided by the MCA algorithm (the data are the rows of the matrix $\mathbf{R} = [Rmi]$ representing the 7 component vector-skill of the models). The HAC clusters the models according to their similarities (based on the Khi2 distance). The HAC used in the MCA analysis yields the following dendrogram (not shown in the paper):
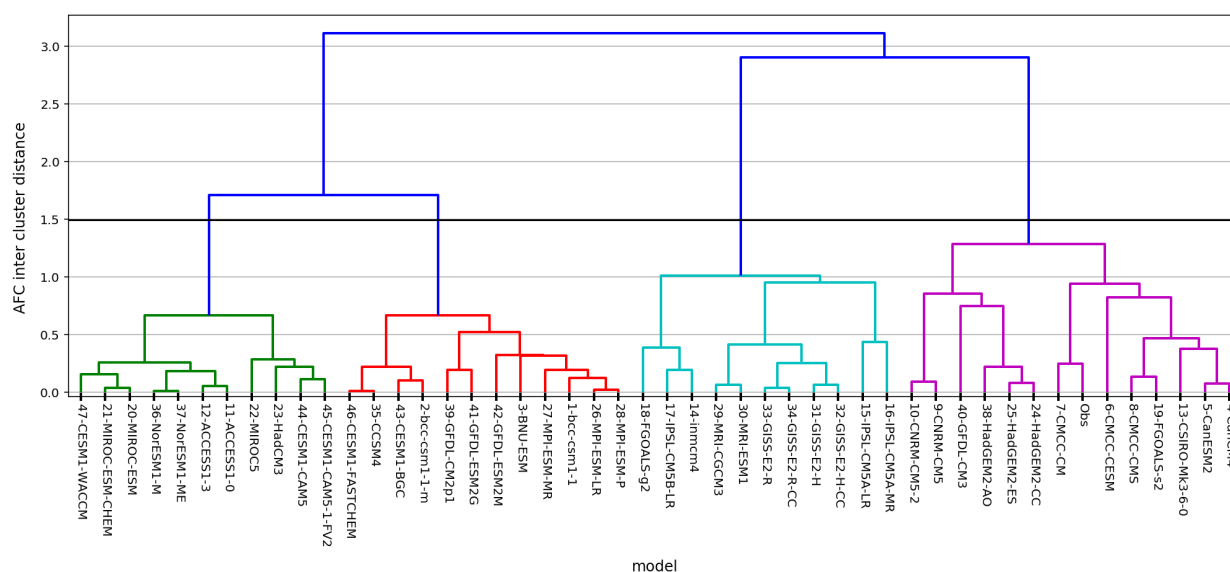

Figure: HAC dendrogram

On the horizontal line, we have displayed the 47 CMIP5 models, each model being associated with its 7 component skill-vector. As the dendrogram represents a hierarchy of clusters, the numbers on the y axis give the distance between two clusters; Clearly there is an optimal jump on this graph: for 4 clusters we obtain well separated Model-groups that are very different. The horizontal black line materializes this optimal jump on the figure (level 1.5 in the vertical axis).. The purpose of this explanation is to highlight the rationality of the selection. We reckon that there is subjectivity in the choice of the approach of the statistical tool, and also in the use of the geophysical knowledge of the region. But by themselves, these tools rely on rational criteria.

. This is presented as a "model weighting" paper, and while that might be possible with this algorithm, I do not believe that is where the strength of the analysis lies.

It was not our intention to present this study as a "model weighting" one. Although model weighting strategies are indeed presented in the introduction, the text only refers to model selection. We have carefully proofread the text so as to make sure to remove this misleading message
We indeed agree with the fact that we do not determine a weighted ensemble model but an ensemble model that better represents the observations than Model-all, which is the mean of all the CMIP5 models we have considered, and also better than the other Model-groups. Our model selection is based on the distance separating the models to the observations .
This combination is provided by the MCA which deals with the 7 component skill-vector associated with each model (and permits to determine a distance to the observation field also associated with a 7 component skill vector) which is more informative than the average skill which has one component only.
Our paper is a "model selection" one.

The paper would be better re-cast as a model analysis paper, using an interesting and useful algorithm to explore the dynamical deficiencies of the models in the region, and informing climate modellers of those deficiencies. I think if the authors wish it to be a model weighting paper, then more emphasis needs to be given to the meaning and justification of the weighting scheme. Further, the authors should develop placing the weighting scheme in the context of established work on the meaning of multi-model ensembles.

We agree with the reviewer that our methodology provides rich and objective information about climate models performance in a specific region. This is one outcome of our study (mainly section 3) and we have strengthened this message in the text and in the conclusion. Nevertheless, We do not agree with the suggestion of the reviewer that the paper is a model analysis paper. Section 4 indeed provides a way (through the MCA) to use a 7 component skill vector to obtain an efficient combination of climate models leading to an efficient multi-model. (Efficient means that its skill is better than the one of Model-all).
 Another question may arise, which is far beyond the objective of the present paper: Is model weighting the best strategy to obtain the most efficient multi-model? Or should we envisage statistical combinations based on multi-parameter analyzes as those developed in the present study?.
In our view, the major contribution of our paper can be summarized into the following sentences included in section 7 (discussion and conclusion):

"The extraction of information embedded in the vector-skill whose 7 components are the skills associated with the 7 sub-regions and the resulting efficient multi-model combination imply the use of advanced statistical tools such as the MCA. Moreover, the study of the vector skill also permits to separate information provided on large offshore ocean circulation from those

occurring in the upwelling region leading to diagnose the deficiencies of some climate models with respect to the modelling of physical processes. Another contribution of the MCA is the visualization of the 47 models and the observations on the plane constituted by the first two MCA axes, which represents 70% of the information embedded in the data. The similarities of the climate models with respect to the observations and the region-clusters are well evidenced. The 'mean' skill associated with each climate model and proposed in this study is easy to use but is far less informative than the vector-skill whose 7 components are the skills associated with the 7 sub-regions. "

We would like to thank again the reviewer for these comments that helped us improve the paper.

Towards an objective assessment of climate multi-model ensembles. A case study : the Senegalo-Mauritanian upwelling region

Juliette Mignot[1], Carlos Mejia[1], Charles Sorror[1], Adama Sylla[1,2], Michel Crépon[1] and Sylvie Thiria[1,3].

[1] IPSL-LOCEAN, SU/IRS/CNRS/MNHN, Paris, France
[2] LPAO-SF, ESP, UCAD, Dakar, Sénégal
[3] UVSQ, F-78035, Versailles, France

Correspondence to: Juliette Mignot (Juliette.mignot@locean-ipsl.upmc.fr)

Abstract. Climate simulations require very complex numerical models. Unfortunately, they typically present biases due to parameterizations, choices of numerical schemes, and the complexity of many physical processes. Beyond improving the models themselves, a way to improve the performance of the modeled climate is to consider multi-model combinations. In the present study, we propose a method to select the models that yield an efficient multi-model ensemble combination. We used a neural classifier (Self-Organizing Maps), associated with a multi-correspondence analysis to identify the models that represent some target climate property at best. We can thereby determine an efficient multi-model ensemble. We illustrated the methodology with results focusing on the mean sea surface temperature seasonal cycle over the Senegalo-Mauritanian region. We compared 47 CMIP5 model configurations to available observations. The method allows us to identify an efficient multi-model combination of 12 climate models. The future decrease of the Senegalo-Mauritanian upwelling proposed in recent studies is then revisited using this multi-model selection.

1- Introduction

In this study, we present a methodology aiming at selecting a coherent sub-ensemble of the models involved in the Climate Model Intercomparison Project, Phase 5 (CMIP5) that best represents specific observed characteristics. The analysis is performed on the capacity of the models to represent the seasonal cycle of the sea surface temperature (SST) in the region of the Senegalo-Mauritanian upwelling off the west coast of Africa.

1   The Senegalo-Mauritanian upwelling has focused increasing attention over the recent
2   years. It presents an important seasonal cycle associated with mesoscale patterns whose
3   variability has been recently studied by several oceanographic campaigns (Capet et al., 2017;
4   Faye et al., 2015; Ndoye et al., 2014). The very productive waters associated with the upwelling
5   have a strong economic impact on fisheries in Senegal and Mauritania, and a crucial societal
6   importance for local populations. It is therefore of importance to predict the evolution of the
7   dynamics and the physics of the upwelling in the forthcoming decades due to the effect of
8   climate warming and its consequences on biological productivity which may impact the
9   fisheries.

10   The most common way to predict the evolution of the climate is to run climate models
11   that include fully coupled atmosphere-ocean-cryosphere-biosphere modules. Because of their
12   quite low resolution and the fact that they use different parameterizations of the physics,
13   numerical schemes and sometimes include or neglect different processes, these models have
14   some marked biases in specific regions. They also have different responses to an imposed
15   increase of atmospheric greenhouse gases, which partly explain their mean climate biases. This
16   variety of models allows us to assess the uncertainty of present climate representation when
17   compared to observations and, by studying their dispersion, to roughly estimate the uncertainty
18   of the response to future climate change.

19   For several generations of climate models, it has been shown that for a large variety of
20   variables the multi-model average mostly agrees better with observations of present day climate
21   than any single model, and that the average also consistently scores higher in almost all
22   diagnostics (Lambert and Boer, 2001; Phillips and Gleckler, 2006; Reichler and Kim, 2008;
23   Santer et al., 2009; Tebaldi and Knutti, 2007). Several studies also suggest that the most reliable
24   climate projection is given by a multi-model averaging (Knutti et al., 2010), rather than
25   averaging different projections performed with a single model run with different initial
26   conditions for example. This result relies on the assumption that if choices of parameterizations,
27   specific numerical schemes, are made independently for each model, then the errors might at
28   least partly compensate, resulting in a multi-model average that is more skillful than its
29   constitutive terms(Tebaldi and Knutti, 2007). The significant gain in accuracy can be explained
30   by the fact that the errors specific to each model compensate each other in the averaging
31   procedure used to build the multi-model. However, the number of GCMs available for climate

change projections is increasing rapidly. For example, the CMIP5 archive (Taylor et al., 2012), which was used for the fifth IPCC Assessment Report (Stocker et al., 2013), contains outputs from 61 different GCMs and 70 contributions are expected for CMIP6. Nevertheless, these models constitute a fully independent ensemble (e.g. Masson and Knutti, 2011). It thus becomes possible and probably needed to select and/or weigh the models constituting such an average. Recent work has suggested that weighting the multi-model averaging procedure could help to reduce the spread and thus uncertainty of future projections. Such an approach has been applied extensively to the issue of climate sensitivity (Fasullo and Trenberth, 2012; Gordon et al., 2013; Huber and Knutti, 2012; Tan et al., 2016). Valuable improvement of models selection has also been found in studies of the carbon cycle (Cox et al., 2013; Wenzel et al., 2014), the hydrological cycle (Deangelis et al., 2015; O'Gorman et al., 2012), the Antarctic atmospheric circulation (Son et al., 2010; Wenzel et al., 2016), extratropical atmospheric rivers (Gao et al., 2016) atmospheric and ocean heat transports (Loeb et al., 2015), the European temperature variability (Stegehuis et al., 2013) and temperature extremes (Borodina et al., 2017).

The present paper is dedicated to the elaboration of an objective method to select models according to their performance over the Senegalo-Mauritanian upwelling area, with the aim of constructing an efficient climate multi-model combination together with its related confidence interval in order to anticipate the effect of climate warming by the end of the century in this region. This upwelling is very intense and presents a well-marked seasonal variability. Its intensity is stronger in boreal winter and it disappears in summer with the northward progression of the ITCZ. Due to the enrichment of the sea surface layers with nutrients upwelled from deep layers, it drives an important phytoplankton bloom that is observed on ocean color satellite images (Demarcq and Faure, 2000; Farikou et al., 2015). The maximum intensity of this bloom occurs in March-April (Farikou et al., 2015; Faye et al., 2015; Ndoye et al., 2014). This upwelling lies at the southern end of the Canarian upwelling system, which has itself a much weaker seasonality and is maximum in summer. Consequently, the Senegalo-Mauritanian upwelling is characterized by a very specific seasonality which is observed on satellite SST (Demarcq and Faure, 2000; Sawadogo et al., 2009). Sylla et al., 2019) have recently shown that the intensity of the SST seasonal cycle along the coast of Senegal and Mauritania was a good marker of the upwelling in climate models. The method we have developed is based on the capability of the climate models to reproduce the SST seasonal cycle observed during the

historical period in key sub-regions. These sub-regions are identified by a neural classifier. The method leads us to rank the different models and to determine an efficient multi-model combination for the analysis of the Senegalo-Mauritanian upwelling and projections of its behavior in global warming conditions.

The paper is articulated as follows: section 2 presents the different climate models and the climatological observations used in the study, together with the region of interest. The classification method is described in section 3 and applied to the extended region. Section 4 presents a qualitative analysis able to group the different climate models in clusters presenting similar performances. Section 5 investigates the results of the method applied over a smaller area, more focused over the upwelling region. Section 6 uses the two multi-model clusters defined in sections 4 and 5 respectively to tentatively predict the representation of the Senegalo-Mauritanian upwelling changes under global warming. Conclusions are given in section 7.

2- Climate Models and region of interest

2.1 Data

This study is based on the CMIP5 (Coupled Model Inter-comparison Project Phase 5) database. We used the output of the 47 simulations listed in Table 1. The models were evaluated over the historical period defined as [1975-2005] by comparing their output to observations. The mean seasonal cycle of SST anomalies over this period is constructed for each model grid point as the difference between the monthly mean temperature and the mean annual temperature. When several members of historical simulations are available for a specific model configuration, they are averaged together. However, this has practically no impact on the estimated mean seasonal cycle (not shown). The mean climatological cycle of the CMIP5 models under study is evaluated against the Extended Reconstructed Sea Surface Temperature data set (ERSST- v3b, Smith et al., 2008), averaged over the same time period. This data set is produced by NOAA at 2° spatial resolution. It is derived from the International Comprehensive Ocean–Atmosphere Dataset with missing data filled in by statistical methods. This dataset is used as the target to be reproduced and is denoted "observation field" hereinafter. In order to deal with data at the same resolution, all model outputs as well the observation fields were regridded on a 1-degree resolution regular grid prior to analysis. A previous study (Sylla et al., 2019) has compared the performance of this

1   dataset as compared to the gridded SST data set from the Met Office Hadley Centre HadISST

2   (Rayner, 2003). Although differences are relatively weak, a subsequent study should analyze the

3   sensitivity of the method to the choice of the target dataset.

4   In section 6, the models' selections are used to characterize the response of the upwelling to

5   climate change. This response is characterized in terms of SST anomalies but also wind intensity.

6   For this, the simulated wind stress is compared to the TropFlux reanalysis. This data set

7   combines the ERA-Interim reanalysis for turbulent and long-wave fluxes, and ISCCP

8   (International Satellite Cloud Climatology Project) surface radiation data for shortwave fluxes.

9   This wind stress product is described and evaluated in (Praveen Kumar et al., 2011).

10

11   **2.2 The Senegalo-Mauritanian upwelling region**

12   In the present research, we evaluated the ability of the different climate models to represent the

13   Senegalo-Mauritanian upwelling. Following (Sylla et al., 2019), we consider the intensity of the

14   seasonal cycle of the SST anomaly as a marker of the upwelling variability and localization. This

15   variable is shown in Fig. 1 for the eastern tropical Atlantic. This figure confirms that the

16   Senegalo-Mauritanian coast stands out with a very strong seasonal SST cycle as compared to

17   what is found at similar latitudes in the open ocean. This results from the cold SST generated by

18   the strong winds occurring in winter. The Senegalo-Mauritanian upwelling is confined in a small

19   region of the order of 100km off the western coast of Africa. It is part of a complex and fine

20   scale regional circulation system recently revisited by Kounta et al., 2018. Since the grid mesh of

21   most of the climate models is of the order of 1° (~100km), this regional circulation is thus poorly

22   resolved, and this pleads for a relatively large-scale analysis of the upwelling representation in

23   climate models. The Senegalo-Mauritanian upwelling is also embedded in a large scale oceanic

24   circulation pattern, encompassing the North Equatorial Counter Current flowing eastward in the

25   southern part of the region and the return branch of the subtropical gyre in the northwestern part.

26   Therefore, we will firstly study the representation of the SST seasonal cycle intensity in the

27   different climate models over a relatively large region that includes part of the Canary current in

28   the North and the Guinea dome in the South. The so-called "extended region" is defined by a

29   rectangular box extending from 9°W to 45°W and from 5°N to 30°N (Fig. 1). In a second step,

30   we will proceed to the same analysis and classification of the models within a much more

focused (hereafter zoomed) region, namely [16°W-28°W and 10°N-23°N] (Fig. 1). All the results below will be first shown for the extended region. Comparison with the focused region will be done in section 4.

3 - Comparing observations and models: a methodological approach

The methodology we have developed is based on the ability of the climate models to adequately reproduce the climatology of the seasonal cycle of the SST anomalies as observed during the last three decades in key sub-regions of the studied domain. These key sub-regions were determined from the similarity of their physical and statistical characteristics through an unsupervised classification, which clusters pixels having similar observed seasonal SST climatology. We chose to deal with a neural classifier, the so-called self-organizing map (SOM hereinafter) developed by Kohonen, 2013 followed by a Hierarchical Ascendant Clustering (HAC, Jain and Dubes, 1998). This method leads to a dynamically interpretable classification. The SOM determines a vector quantization of the dataset, which compresses the initial dataset into a relatively small number of referent vectors. Doing so allows to take the non-linearities of the dataset into account and to filter the noise, which can make the classification spurious. This reduced number of dataset vectors enables an HAC to determine the highly non-linear borders between the different SOM clusters. This procedure has been used with success in several studies (Farikou et al., 2015; Jouini et al., 2016; Niang et al., 2003, 2006; Sawadogo et al., 2009). Note that the use of an HAC directly on the initial dataset would not be efficient in the present study because the number of degrees of freedom (here the grid points of the initial domain) is too large for this method to work efficiently. In the present section, we describe the methodology we developed to score the different climate models with respect to the observations. In section 4, we will tentatively group the different climate models into blocks having the same behavior by using a Multiple Correspondence Analysis (MCA in the following).

3.1 The unsupervised classification method

The first step of the methodology was to decompose the selected region in different classes (the key sub-regions mentioned above) by using a neural network classifier, the so-called SOM (Kohonen, 2013). This algorithm constitutes a powerful nonlinear unsupervised classification

method. It has been commonly used to solve environmental problems (Hewitson and Crane, 2002; Jouini et al., 2013, 2016; Liu et al., 2006; Reusch et al., 2007; Richardson et al., 2003). The SOM aims at clustering vectors (here the 12 SST seasonal anomalies) of a multidimensional database (D) (here the grid points of the studied domain) into classes represented by a fixed network of neurons (the SOM map). The self-organizing map (SOM-map) is defined as an undirected graph, usually a 2D rectangular grid. This graphical structure is used to define a discrete distance (denoted by δ) between the neurons of the map and thereby identify the shortest path between two neurons. Moreover, SOM enables the partition of D in which each cluster is associated with a neuron of the map and is represented by a prototype that is a synthetic multidimensional vector (the referent vector w). Each vector z of D is assigned to the neuron whose referent w is the closest, in the sense of the Euclidean Norm (EN), and is called the projection of the vector z on the map. A fundamental property of a SOM is the topological ordering provided at the end of the clustering phase: two neurons that are close on the map represent data that are close in the data space. In other words, the neurons are gathered in such a way that if two vectors of D are projected on two "relatively" close neurons (with respect to δ) on the map, they are similar and share the same properties. The estimation of the referent vectors w of a SOM and the topological order is achieved through a minimization process using a learning data set base, here from the observations. The cost function to be minimized is of the form:

$$J_{SOM}^{T}(\chi, W) = \sum_{zi \in D} \sum_{c \in SOM} K^{T}(\delta(c, \chi(z_i)))\|z_i - w_c\|^2$$

where $c \in SOM$ indices the neurons of the SOM map, χ is the allocation function that assigns each element z_i of D to its referent vector $w_{\chi(z_i)}$ and $\delta(c, \chi(z_i))$ is the discrete distance on the SOM-map between a neuron c and the neuron allocated to observation z_i. K^T a kernel function parameterized by T (where T stands for "temperature" in the scientific literature dedicated to SOM) that weights the discrete distance on the map and decreases during the minimization process. At the end of the learning process, the classification can be visualized onto the SOM-map and interpreted in term of geophysics.

3.2 - Classification of the observations

In the present problem we chose to classify the annual cycles of the SST seasonal anomalies observed in the Senegalo-Mauritanian upwelling. The study was made over the "extended

1   region" constituted of 25 x 36 = 900 pixels, but this enlarged region covers a part of the African

2   continent and 157 pixels are in fact over land. That means that we have truly 743 ocean pixels to

3   deal with. We consider the time-period of 30 years [1975 to 2005] extracted from the ERSST-V3b

4   database. For a given grid point and a given year and month, the monthly anomaly is the SST of

5   the pixel for which we have subtracted the mean of the considered year. The climatological mean

6   of the anomaly is then computed for each grid point by averaging each climatological month

7   over the 30 years. Thus, the learning data set D is a set of 743 twelve-component vectors z, each

8   component being the mean monthly anomaly computed as above. We denote "SST seasonal

9   cycle" the vector z in the following.

10   We used a SOM-map to summarize the different SST seasonal cycles present in the "extended

11   region". We found that 120 prototypes (or neurons) can accurately represent the 743 vectors of

12   D. This reduction (or vector quantization) is made by using a rectangular SOM-map of 30 x 4

13   neurons.

14   We then reduced the number of neurons in order to facilitate their interpretation in terms of

15   geophysical processes. For this, we applied a Hierarchical Ascendant Clustering algorithm

16   (HAC) using the Ward dissimilarity (Jain and Dubes, 1988). We grouped the 120 neurons of the

17   SOM into a hierarchy that can contain between 1 and 120 clusters. Then the different

18   classifications proposed by the HAC were applied to the geographical region: each SST seasonal

19   cycle of each grid point of the region is assigned to a neuron and consequently to a cluster

20   (assignment process), thereby defining the so-called region-clusters. The problem is then to

21   choose a number of clusters that adequately synthesizes the geophysical phenomena over the

22   region. This was done by looking at the different possible classifications and choosing one

23   representing the major characteristics of the upwelling region. In Fig. 2a, we observe that when

24   we partition the SOM in 7 clusters, the associated 7 region-clusters are constituted of contiguous

25   pixels in the geographic map, and that two clusters (6, 7) are within the upwelling region and

26   present a well-marked seasonal cycle. For each region-cluster, we estimated the monthly mean

27   of the SST seasonal cycle and the associated spread captured by the neurons constituting this

28   region-cluster.

29   The typical SST climatological cycles for each region-cluster are presented in Fig. 2b

30   together with their related error bars. We note that the region-clusters are well identified, their

typical climatological annual cycles of SST being well separated. Furthermore, the 7 region-clusters are spatially coherent and have a definite geophysical significance.

For the extended region under study, 7 therefore appears to be an adequate cluster number, since this number allows a clear partition of the clusters on the HAC decision tree on the one hand, and permits to assign a clear physical significance to each region-cluster on the other hand. the Senegalo-Mauritanian coastal upwelling is associated with clusters 7 and 6. Cluster 2 corresponds to deep tropical waters associated with the equatorial Countercurrent. Cluster 1 corresponds to surface waters of the Gulf of Guinea. Cluster 3 corresponds to the offshore tropical Atlantic, and cluster 5 has extratropical characteristics. Cluster 4 is transition between 3 and 5. As expected, the equatorial regions (clusters 1 and 2) have a very weak seasonal cycle, which increases towards the extratropics (clusters 3 to 5). The upwelling regions (clusters 6 and 7) are characterized by an exceptionally strong seasonal variability.

3.3 – Classification of the climate models over the extended upwelling region

The aim is now to find the model(s) that best fit the "observation field". A heuristic manner is to compare the pattern of the different region-clusters of the CMIP5 models with respect to those of the "observation field" through a sight evaluating process. This kind of approach has been proposed in Sylla et al., 2019, and we indeed immediately see that some models better fit the "observation field" than others. But this method remains very subjective.

In the following, we present a more objective approach. We use the previous classification to objectively estimate how each CMIP5 model fits the "observation field" and its seven region-clusters. For this, we projected the SST annual cycle of each CMIP5 model grid point of the extended region onto the SOM learned with the observations (section 3.2) using the assignment procedure described in this section. Each grid point thus corresponds to a cluster of the SOM and is represented on the geographical map by its corresponding color. Doing so, we can represent each CMIP5 model by the geographical pattern of the 7 clusters partitioning the SST seasonal cycle of its grid points. The geographical maps representing the 47 models and their associated clusters are plotted in Fig. 3. This graphical visualization is easier to compare than the original characteristics (amplitude and phase) of the annual cycle at each grid point of a model since each grid point can only take one discrete value among seven. This representation immediately allows identifying the model biases and the models that best reproduce the cluster-

1 regions identified in the observations. A huge amount of information could in principle be

2 extracted from these maps, both from individual modelling groups, to understand the

3 representation of this region by the models and origins of possible biases, and from experts of the

4 area, to understand the difficulties of the climate models to represent the SST seasonal cycle in

5 this region.

6   For a more quantitative assessment, we counted the number of grid points of a region-

7 cluster for a given CMIP5 model matching the same region-cluster of the "observation field".

8 We then computed the ratio between that matching number and the number of pixels of the

9 region-cluster of the considered model. That number is noted in the color-bar for each region-

10 cluster in Fig. 3. We denote Rmi the ratio for the region-cluster i and the model m, where

11 $i = 1, …, 7$ is the number of the region-cluster and m $= 1, …, 47$ is the number of the model (see

12 table 1). We note that R$mi \leq 1$. Doing so, each model m is represented by a 7-dimensional

13 vector Rm, each component being the ratio of a region-cluster. We estimated the total skill of a

14 model by averaging the 7 ratios. Note that this procedure gives the same weight to each region-

15 cluster whatever its number of grid points and its proximity with the upwelling region. In the

16 following the skill is presented as a percentage, the higher the skill, the better the fit. In Fig. 3,

17 the 47 CMIP5 models are ranked by their total skill, which is indicated above each panel beside

18 the model name. The model skills are very diverse, ranging from 79% to 28%. This figure also

19 shows that the models presenting the best total skill are also those representing thoroughly the

20 upwelling region. Some models represent the large-scale structure in the eastern tropical Atlantic

21 (region-clusters 3, 4, 5) very well but not the upwelling (33-GISS-E2-R and 34-GISS-E2-R-CC

22 for example). Others represent pretty well the upwelling region-clusters (region-clusters 6 and 7),

23 but not the large-scale structures of the SST seasonality (13-CSIRO-Mk-3-6-0, 6-CMCC-CESM

24 for example). None of these models is ranked among the best models, with a score greater than

25 60%. As indicated above, this representation gives a very synthetic view of the structure of the

26 seasonality of the SST cycle in each of the models, potentially a very useful guide for climate

27 modelers to identify rapidly major biases.

28

29 **4 – Qualitative analysis of the climate models**

1   In order to further progress in the selection of the models, the 47 climate models and the
2   observation field were then analyzed by using a Multiple Correspondence Analysis (MCA in the
3   following). MCA is a multivariate statistical technique that is conceptually similar to principal
4   component analysis (PCA in the following), but applies to categorical rather than continuous
5   data. Similarly as PCA, it provides a way of displaying a set of data in a two-dimensional
6   graphical form.

7   In the following, we apply a MCA analysis to the (47,7) matrix $\mathbf{R}$ = [Rm_i] whose
8   elements represent the skills of the clusters of the models shown in front of the color bars in Fig.
9   3: the rows m represent the 47 different models, the columns i the 7 region-clusters. The MCA,
10   as the PCA, projects the initial matrix on a new basis in such a way that the new axes are the
11   matrix eigenvectors (PC), the inertia of each axis being the corresponding eigenvalues.
12   According to the theory, the MCA matrix analysis of R gives i-1 = 6 independent PCs. Each
13   model is thus now associated with a 6-dimensional vector on which it has a specific weight. The
14   MCA uses for this analysis the khi-2 distance. In figure 4, we present the projection of the
15   models and the "region clusters" in the plane formed by the two first axes (x=PC1 and y= PC2)
16   of the MCA. These two axes represent 70 % of the total inertia. Each model is represented by a
17   small circle and each region-cluster by a purple square. Moreover, we projected the observation
18   field (green diamond) on that plane as a supplementary individual. To have a more precise view
19   of the topology, it would be necessary to consider the projection on the 5 other PCs, which
20   represent 30% of the inertia.

21   In the (PC1, PC2) plane, the shorter the distance between two models, the more similar
22   the distribution of their region-cluster skills. Proximity between a model and a region-cluster
23   leads us to affirm that this region-cluster is well represented by that model. Clearly, some models
24   adequately represent the southern part of the extended region (region-clusters 1, 2 or 3), where
25   the SST seasonal cycle is weak, and are very distant from the upwelling regions (region-cluster 6
26   and region-cluster 7) whose large SST cycle is poorly reproduced. In this group of models, one
27   recognizes the model 16-IPSL-CM5A-MR, at the extreme bottom of Fig. 4, close to region-
28   clusters 4 and 5, consistently with Fig. 3. At the other end of this group of models, the model 23-
29   HadCM3 for example is located very close to the region-cluster 1. Fig. 3 indeed shows that most
30   of its grid points over the region of interest have a seasonal cycle resembling the one found in the

1   offshore tropical ocean. Another group of models is located in the center of this plan, thus at an

2   optimal distance of each of the observed regions-clusters, and not far from the overall position of

3   the observations (diamond). We recognize in this group of models those that have a high skill in

4   Fig. 3. The positioning of the observations (green diamond in Fig. 4) with respect to the models

5   indeed allows selecting those that best represent the observations field. The representation given

6   in Fig. 4 allows understanding the drawback of the different models with respect to the 7 Modes

7   of SST-cycles.

8   As indicated in the introduction, the main objective of the methodology is to select an

9   ensemble of models that represents at best the upwelling behavior with respect to the

10   observations and to use this ensemble to predict the impact of climate change in the Senegalo-

11   Mauritanian upwelling with some confidence. The problem is now to determine a subset of

12   models which has a better skill than Model-All, in other words minimize the distance to the

13   observations. As the number of models is small enough, we chose to cluster them by an HAC

14   according to their projections onto the six axes provided by the MCA, and select the optimal

15   jump in the hierarchical tree (Jain and Dubes, 1988).

16   Doing so, we obtain four homogeneous groups which are well separated (group 1, 2, 3,

17   4). They are plotted with different colors in Fig. 4. We denote Model-group 1, Model-group 2,

18   Model-group 3, Model-group 4 these multi-model ensembles hereinafter. Model-group 4

19   represents the observations and the upwelling region-clusters at best.

20   For each group, we computed a multi-model average whose outputs are the mean of the

21   outputs of its different members and we analyzed it according to the same procedure (projection

22   of the SST-seasonal cycle and assignment to a region-cluster) used for each individual model.

23   Besides we introduced the full multi-model average (Model-All in the following), which is the

24   multi-model ensemble, which averages the 47 CMIP5 model outputs. Model-All was also

25   projected in the MCA plane and it is represented by a red star in Fig. 4. Comparison of the four

26   model-groups with Model-All and the observations are presented in Fig. 5. This figure visually

27   highlights the dominance of Model-group 4 for the reconstruction of the SST seasonal cycles of

28   the different region-clusters for the extended region. This is particularly clear for region-clusters

29   6 and 7, which are those located in the upwelling region (Fig. 2). Model-group 3 seems to group

30   models characterized by an equatorward shift of the main structures, since the region-cluster 1 of

1   tropical waters is not reproduced and Region-clusters 4 and 5 of extratropical waters are

2   overestimated. Fig. 4 indeed shows that this Model-group is very close to the Regions-clusters 4

3   and 5, which correspond to the extratropical and the transition geographical regions. Model-

4   group 2 misrepresents the region of the Canary upwelling. Model-group 1 overestimates the SST

5   seasonal cycle in all the tropical open Atlantic. These two last model-groups overestimate the

6   region-Cluster 1, again consistently with their position in Fig. 4. A detailed physical

7   interpretation of the Model-groups is nevertheless beyond the scope of this paper. Clearly

8   Model-All represents the SST seasonal cycle of the off-shore ocean, but it proposes a very poor

9   representation of the upwelling region.

10   Two models (models 7 and 25) have a better skill than Model-group 4 and Model-All.

11   These two models are very close to the observations on the first two axes of the MCA (Fig 4). It

12   is easily seen that Model-group 4 and the projection of Model-All on this plane is farther than

13   that of model 7 and model 25 from the observation projection. This explains the lower

14   performance of these two multi-models as compared to models 7 and 25. In the present case, the

15   method permits to determine the best models (model 7 and model 25) and to outline the best

16   multi-model (Model-group 4) whose skill is better than any model with a probability of 95%

17   (number of models whose skill is smaller than the skill of Model-group 4 with respect to the total

18   number of models). Projection of the models on the other planes of the MCA analysis should

19   confirm this interpretation. One could then question the use of Model-group 4 rather than model

20   7 or model 25 individually. Furthermore, we argue that multi-model averages are in general more

21   robust for climate studies than the use of a single model that can have good performance for a

22   very specific set of constraints but not for neighboring ones. The following section will partly

23   justify this point.

24

25   **5 - Analysis of the climate models over a zoomed upwelling region**

26   The classification presented above relies largely on the ability of the models to represent

27   the off-shore seasonal cycle of the SST. In the following, we propose to test the classification

28   over a much more reduced area in order to focus the analysis on the upwelling area. This

29   "zoomed upwelling region" is shown in Fig. 1.

30   As for the extended region, we partitioned the observations of the zoomed upwelling

31   region with a SOM (ZSOM in the following) followed by a HAC. We then applied a new MCA

to regroup the climate models. We did a similar analysis as this performed in section 4. We obtained four new region-clusters well separated denoted ZRegion-clusters. Fig. 6 shows the four ZRegion-clusters obtained from ERSSTv3b observations together with their associated mean SST seasonal cycle. Again, the ZRegion-clusters are spatially coherent. The upwelling area is now decomposed into three ZRegion-clusters (ZRegion-clusters 2, 3, 4). This new decomposition thus refines the study performed for the extended region: ZRegion-cluster 1 represents the offshore ocean: its grid points typically have a SST seasonal cycle amplitude of 4°C, very similar to Region-cluster 4 in the classification performed over the extended region (Fig. 2). ZRegion-cluster-4 nicely identifies the core of the Senegalo-Mauritanian region, with grid points characterized by the greatest amplitude of the SST seasonal cycle of the domain: typically 6.5°C. It is interesting to note that an additional upwelling ZRegion-cluster (ZRegion-cluster 3) appears south of ZRegion–cluster 4. Indeed, several studies have shown that the Cape Verde peninsula, located around 15°N, separates the upwelling region into two distinct areas having a different behavior north and south of this peninsula (Sirven et al., 2019; Sylla et al., 2019). The location of the separation between ZRegion-cluster 3 and 4 is determined with some uncertainty due to the coarse resolution (1°) of the ocean models. ZRegion-cluster 3 is marked by a time shift of the seasonal cycle: the warmest season seems to occur somewhat one month earlier than in the other regions as clearly seen in Fig. 6 (left panel, yellow curve in June). Due a classification done in a much larger region, such characteristic does not appear in the study over the extended area study. The physical interpretation of the SST seasonal cycle of this ZRegion-cluster is beyond the scope of the present study, but one can suspect a role of the ITCZ seasonal migration, covering these grid points earlier than further north. Finally, ZRegion-cluster 2 is a transition between the large scale ocean and the upwelling region.

As for the extended region, we applied a MCA analysis to the (47 x 4) matrix R = [Rmi] whose elements represent the skills of the four clusters (i) of the 47 models. This MCA was followed by a HAC leading the definition of five ZModel-groups. The members of each group are given in appendix. Fig. 7 shows the ZRegion-cluster obtained in the zoomed area by projecting these five ZModel-groups and Model-All model on the ZSOM and their associated performances. ZModel-group 1 is the least performing one: only 25% of the grid cells fall in the same class as for the observations. The structure of this model-group shows that it is characterized by an homogeneous amplitude of the seasonal cycle over the whole domain,

suggesting a largely reduced upwelling: only one grid point at the coast has an enhanced SST seasonal cycle as compared to the large scale tropical ocean. ZModel-group 2 is the best performing one: 66% of the grid points are assigned to the correct class and the general picture indeed represents a four-class picture fairly consistent with the observed structure (Fig. 6). Important biases yet remain. In particular, the ZRegion-clusters 2 and 4 characterizing the upwelling extend too far offshore. The three other ZModel-groups are intermediate. A relatively reduced upwelling area, with an underestimated SST seasonal cycle, characterizes ZModel-groups 3 and 4. ZModel-group 5 corresponds to a shift of the upwelling region towards the north. Model-All also shows a strongly reduced seasonal cycle, with a large amount of pixel in the intermediate ZRegion-cluster 3 and very few in the ZRegion-cluster 4. The ZRegion-cluster 3 representing the southern part of the Senegalo-Mauritanian upwelling does not appear in the pattern of Model-All.

We remark that all the models forming ZModel-group 2 are included in Model-group 4. For a more precise assessment, we can also project the entire Model-group 4, identified as the best multi-model ensemble over the extended region, on the ZSOM (Fig. 8, right). We notice that the performance of Model-group 4 remains very high on this projection, indicating some robustness of this multi-model ensemble. Moreover, this ensemble now outperforms the single best model identified over the extended region (Fig. 8, left). This result gives further confidence in the use of multi-model averages, illustrating that one single model can be very skillful over a specific region, or for a specific analysis, but multi-model averages are more robust across various analysis and/or regions.

6 – Impact of climate change on the Senegalo-Mauritanian upwelling

6.1 Representation of the upwelling in the CMIP5 climate models clusters

In this section, we compare the representation of the Senegalo-Mauritanian upwelling system given by the two best Model-groups identified above (Model-group 4 and ZModel-group 2). For this evaluation, we use two of the five indices used by (Sylla et al., 2019) to evaluate the full database, namely the intensity of the SST seasonal cycle and the offshore Ekman transport at the coast. The former is specific to the seasonal variability of the Senegalo-Mauritanian upwelling system, and it has been used for the classification. The latter is more general and although it has recently been shown to partly represent the volume of the upwelled waters (Jacox et al., 2018), it is extensively used in the scientific literature to characterize upwelling regions (Cropper et al.,

1   2014; Rykaczewski et al., 2015; Wang et al., 2015). Note also that following Sylla et al., 2019,

2   evaluation is performed on the period [1985-2005]. This period slightly differs from the

3   classification period but the SST seasonal cycle is not significantly different (not shown).

4   Fig. 9 compares the amplitude of the SST seasonal cycle as represented in the

5   observations, Model-All, Model-group 4 and ZModel-group 2 identified above. Consistently

6   with Fig. 5 and 7, Model-All dramatically underestimates the upwelling signature in terms of

7   SST seasonal cycle as compared to the observations. Model-group 4 and ZModel-group 2 yield

8   improved results: the area of enhanced SST seasonal cycle is larger both in latitude and

9   longitude, with stronger SST amplitude values. This confirms the efficiency of the selection

10   operated above. Nevertheless, ZModel-group 2 yields a realistic SST amplitude pattern along the

11   coast but it extends too far offshore. Furthermore, in ZModel-group 2, the subtropical area (in

12   green in Fig 9) extends too far towards the south, in particular in the western part of the basin.

13   The tropical area, characterized by limited amplitude of the seasonal (deep blue in Fig. 9), is

14   shifted to the south as compared to the observations. In other words, the large scale thermal, and

15   thus probably dynamical structure of the region is poorly represented in ZModel-group 2.

16   Finally, Model-group 4 is the least biased one.

17   The intensity of the wind stress parallel to the coast, inducing offshore Ekman transport

18   and consequently an Ekman pumping at the coast, is generally considered as the main driver of

19   the upwelling. We therefore also tested the representation of this driver in the different Model-

20   groups. The idea is to evaluate the impact of the model selection performed above on the

21   representation of an independent variable by the Model-groups. Fig. 10 shows the latitude-time

22   evolution of the meridional oceanic wind stress, considering that the coast in the studied region is

23   oriented approximately meridionally, so that the offshore Ekman transport is mainly zonal. Note

24   that in Fig. 10, southward winds have positive values so that they correspond to a westward

25   Ekman transport, favorable to upwelling. Panel (a) shows that the observed meridional wind

26   stress is, all year long, favorable to the upwelling north of 20°N. At these latitudes, it is stronger

27   in summer. Between 12°N and 20°N, in the latitude band of the Senegalo-Mauritanian

28   upwelling, on the contrary, the wind blows southward with a very weak intensity in summer and

29   it even changes direction in the southern part of this latitude band. It is favorable to the upwelling

30   in winter-spring, which explains why the Senegalo-Mauritanian upwelling occurs during this

31   season with a maximum of intensity in March-April (Capet et al., 2017; Farikou et al., 2015).

1 The main bias of Model-All (Fig. 10b) is that the wind stress never reverses between 12°N and

2 20°N. It weakens in the southern part of the Senegalo-Mauritanian latitude band, i.e. south of the

3 Cape Verde peninsula (15°N), but does not become negative. North of the Cape Verde peninsula,

4 it blows from the north also in summer, so that the Senegalo-Mauritanian upwelling lacks of

5 seasonality. This bias is corrected in Model-group 4 and ZModel-group 2 (Fig. 10, panels c and

6 d) that are, in this aspect, more realistic than Model-All. Model-group 4 shows a slight extension

7 of the time and latitude range where the oceanic wind stress reverses sign. This constitutes an

8 improvement. The southward wind is nevertheless too strong in winter over the [12°N-20°N]

9 latitude band as well as further south from December to March. These two remaining biases are

10 further reduced in ZModel-group 2. This latter model yields the most realistic seasonal cycle of

11 meridional oceanic wind stress over the latitude band under study. This is consistent with a very

12 localized model selection, as the wind index is itself localized along the coast.

13 To conclude, Model-group 4 and ZModel-group 2 perform in general better than Model-All in

14 reproducing the major characteristic features of the Senegalo-Mauritanian upwelling. This result

15 confirms the relevance of the multi-model selection we have presented above. Applying the

16 methodology over a relatively large region allows to better constraining the spatial extent and

17 pattern of the SST signature of the upwelling than the reduced area. The latter however yields a

18 better representation of the wind seasonality along the coast.

19 **6.2 Response of the Senegalo-Mauritanian upwelling to global warming.**

20   In this section, we examine the response of the upwelling system given by the different

21 multi-model groups we selected, to global warming. For this, we compared the two indices

22 analyzed above in present-day and future conditions. The present-day conditions are taken as

23 above as the climatological average of historical simulations over the period [1985-2005]. The

24 future period is taken as the climatological average of the RCP8.5 scenario over the period

25 [2080-2100]. Fig. 11 shows the difference of the SST seasonal cycle amplitude between these

26 two periods. The general behavior is that the SST cycle amplitude will reduce in the upwelling

27 region. Sylla et al., 2019 showed that this is primarily due to a warming of the winter

28 temperature, thus suggesting that the upwelling signature in surface will reduce. On the other

29 hand, this figure shows that the upwelling signature will increase along the Canary current,

30 which flows along the coast of Morocco, as well as in the subtropical part of our domain. This

31 behavior is observed in the three multi-model ensembles. Yet, the two selected Model-groups

suggest a weaker decrease of the SST seasonal cycle in the upwelling region than the one given by Model-All. ZModel-group 2 shows an even weaker decrease mainly confined in the southern part of the upwelling region. This result echoes findings of Sylla et al., 2019 based on another indicator of the upwelling imprint on the SST: they showed that the difference between the SST at the coast and offshore is expected to decrease more in the southern part of the Senegalo-Mauritanian upwelling system (SMUS) than in the north . We can hypothesize that the study conducted on the reduced area permits to separate the Senegalo-Mauritanian upwelling system into two clusters, a northern one (ZRegion 4) and a southern one (ZRegion-3) (Fig. 7) which enables to distinguish this specific response.

The meridional wind stress also generally weakens under climate change in the [12°N-20°N] latitude band (Fig. 12), suggesting a general reduction of the upwelling intensity. From December to March, this is particularly true in the southernmost region of the Senegalo-Mauritanian band, consistently with the results of (Sylla et al., 2019). The wind pattern inferred from the two Model-groups (Fig. 12, middle and right panels) present a higher seasonal variability than this of Model-All (left panel). The winter reduction of the southward wind stress is slightly more confined to the southern region in ZModel-group 2, especially at the end of the upwelling season (March-April) when the upwelling intensity is the strongest. This may be consistent with the reduced seasonal cycle in the southernmost part of the upwelling identified above.

7 - Discussion and Conclusion

This paper proposed a novel methodology for selecting efficient climate models over a specific area (here the Senegal-Mauritania upwelling region) with respect to observations and according to well-defined statistical criteria. In the present study, we have specifically checked the ability of the climate models to reproduce the ocean SST annual cycle observed in specific sub-regions of the studied domain during the period 1975-2005 as reported in the ERSST_v3b data set. These sub-regions were defined by a neural classifier (SOM) as clusters having similar seasonal SST cycle anomalies with respect to some statistical characteristics, and were therefore named region-clusters. They correspond to ocean areas having well marked oceanographic specificities.

We then checked the ability of the different climate models to reproduce the region-clusters defined on the observation dataset with a SOM. The better a climate model fits the clusters computed with the SST observation, the higher the skill of the model. To evaluate this, we

1   defined geographical regions in the different CMIP5 climate models by projecting the SST

2   annual cycle anomalies of each model grid point onto the SOM. Each grid point is associated

3   with a cluster on the SOM map and consequently to a region-cluster on the geographical map.

4   We built a similarity criterion by counting the number of grid points in a region-cluster of a

5   given model matching the same region cluster defined by processing the observation field.

6   We then computed the ratio between that matching number and the number of pixels of the

7   region-cluster of the model under study. We estimated the total skill of a model by averaging

8   the 7 ratios associated with the 7 region clusters. Note that this procedure presents the advantage

9   to give the same weight to each region-cluster whatever its number of grid point and its

10   proximity with the upwelling region. This procedure respects the clustering done by the SOM

11   since the different clusters have an equal weight in the skill computation. In its present

12   definition, the total skill is a number between 0 and 1, the higher the skill, the better the fit. Other

13   measures of the total skill of a Model-group could nevertheless be defined depending on the

14   objective of the study. One may compare the skill of individual models over a specific region-

15   cluster of interest, or analyze the pattern of skill in one specific model and its sensitivity to

16   possible various parameterization schemes. The extraction of information embedded in the

17   vector-skill whose 7 components are the skills associated with the 7 sub-regions and the resulting

18   efficient multi-model combination imply the use of advanced statistical tools such as the MCA.

19   Moreover the study of the vector skill also permits to separate information provided on large

20   offshore ocean circulation from those occurring in the upwelling region leading to diagnose the

21   deficiencies of some climate models with respect to the modeling of physical processes. Another

22   contribution of the MCA is the visualization of the 47 models and the observations on the plane

23   constituted by the first two MCA axes, which represents 70% of the information embedded in the

24   data. The similarities of the climate models with respect to the observations and the region-

25   clusters are well evidenced. The 'mean' skill associated with each climate model and proposed in

26   this study is easy to use but is far less informative than the vector-skill whose 7 components are

27   the skills associated with the 7 sub-regions.

28   Such a multi-model ensemble selection indeed allows sampling a set of models in order to obtain

29   a more realistic climatology over the region of interest. The response of the upwelling to climate

30   change given by the different multi-model ensembles is quite robust in the sense that they give

31   similar qualitative answers. However, a too selective ensemble of models may lead to noisy

1   patterns. A compromise thus has to be found between the advantage of using a large number of

2   models, in order to smooth biases and unrealistic patterns, or selecting the most realistic models,

3   with the advantage of using a small number of models in the averaging procedure, but with the

4   possible inconvenience of getting spurious biases.

5   As discussed in the introduction, different criteria have been used for extracting some efficient

6   models from the CMIP5 models used for climatic studies. The most common parameter is the

7   average annual surface mean temperature of the grid points of the region under study.

8   Besides,(Knutti et al., 2006) used the seasonal cycle in surface temperature represented by

9   seasonal amplitude in temperature calculated as summer June–August (JJA) minus winter

10   December–February (DJF) temperature. This criterion is more informative than the annual mean

11   temperature since the amplitude of the seasonal variability is an important criterion

12   characterizing the validity of a climate model. In the present work, we used a much more

13   informative criterion which is formed of the monthly temperature cycle anomaly represented by

14   a 12 components vector, each component representing the average monthly temperature of the

15   year we consider. This new criterion allows taking account the amplitude and the phase of

16   seasonal variability while the Knutti et al., 2006 criterion only takes into account the amplitude

17   of the seasonal variability. Note however that it implies a good geophysical knowledge of the

18   region under interest, in order to determine the relevant region-clusters after the SOM. It is also

19   very specific to the Senegal-Mauritania upwelling region. Furthermore, Sylla et al., 2019

20   extensively discussed the possible differences among several indices aiming at characterizing the

21   upwelling and the need to use some of them to have a complete understanding of this coastal

22   phenomenon. This conclusion is probably general to any physical process of the climate system.

23   In the present study, the model selection is based on only one signature of the SMUS. Several

24   possibilities can be envisaged to improve the resolution of this problem such as merging several

25   indices like SST, temperature at several depths, wind vector, ocean currents,... This approach

26   could also allow a selection of models based on the representation of several distinct regional

27   behaviors. In spite of several subjective choices, including the studied domain and the statistical

28   metrics, we argue that this method is a step towards an objective selection of models, based on a

29   quantitative assessment rather than a qualitative analysis of maps of performance.

30   Different applications of the multi-model selection strategy proposed in the present study can be

31   envisaged. Firstly, from a purely modeling point of view, the projection of the models on the

1   SOM (or ZSOM) and the results of the HAC yield a very enlightening description of a given

2   model behavior in terms of region-clusters of the area under study. In our view, such a procedure

3   could advantageously be used by individual modeling groups to identify, analyze and therefore

4   hopefully reduce their model biases in a targeted region. Secondly, from a physical point of

5   view, an identified Model-group can be used to analyze the targeted region (here the SMUS) in

6   term of processes with the advantages of the multi-model mean in which the constituting models

7   have been selected from quantitative criteria. Such an application has been briefly illustrated by

8   showing how the selected Model-group represents an important additional characteristic of the

9   SMUS, not used for the selection, namely the Ekman pumping. Promising reduction of biases of

10 the full multi-model mean ensemble has been identified, opening perspectives for process studies

11 based on this sub-ensemble of the CMIP5 database. A third application of the selection lies in the

12 prediction of the future climate. Here, we have shown that selected multi-model ensembles may

13 provide a more precise description of the future behavior of the SMUS. It may nevertheless be

14 important to note that these conclusions are based on the assumption that the CMIP5 models

15 which have been selected according to their present-day characteristics, are the most reliable in

16 terms of future projections, which can be questioned and refined (Lutz et al., 2016; Reifen and

17 Toumi, 2009).

18 As discussed in the introduction, the concept of "model democracy", suggesting that all models

19 should be equally considered in multi-model ensemble is now strongly questioned (Knutti et al.,

20 2017). The present study proposes a promising way to improve the quality of multi-model

21 ensemble in terms of model selection. Deep advances in the field of multi-model analysis and

22 selection can be expected from the emerging topic of climate informatics (Monteleoni et al.,

23 2016) as it has been shown through the present study. Artificial intelligence and machine

24 learning may indeed provide efficient tools to make the best out of the extraordinary but

25 imperfect tools that are the climate models and the multi-model intercomparison efforts.

26

the french Institut de Recherche pour le Développement. J.M. was also supported by the H2020-EUCP project under grant agreement 776613. To analyze the CMIP5 data, this study benefited from the IPSL Prodiguer-Ciclad facility which is supported by CNRS, UPMC, Labex L-IPSL which is funded by the ANR (Grant #ANR-10-LABX-0018) and by the European FP7 IS-ENES2 project (Grant #312979)

Code and Data availability: The model output used for this study is freely available on the ESGF database for example following this url: https://esgf-node.ipsl.upmc.fr/search/cmip5-ipsl/. The SST data were downloaded from https://www.esrl.noaa.gov/psd/data/gridded/data.noaa.ersst.v3.html and the winds data here: https://podaac.jpl.nasa.gov . The code developed for the core computations of this study can be found under: 10.5281/zenodo.3476724. This code allows reproducing Fig. 2, 3, 6, 7 and 8.

Author contribution: JM initially proposed the idea, ST and MC translated it in terms of methodology and coordinated the method development, CS and CM developed the code and produced the figures, CS, CM, MC, ST all contributed to the statistical analysis. As provided the initial definition of the upwelling index and performed the analysis under climate change that is presented in section 6. JM, MC and ST prepared the manuscript with contributions from all the authors.

Références

Borodina, A., Fischer, E. M. and Knutti, R.: Potential to constrain projections of hot temperature extremes, J. Clim., 30(24), 9949–9964, doi:10.1175/JCLI-D-16-0848.1, 2017.

Capet, X., Estrade, P., Machu, E., Ndoye, S., Grelet, J., Lazar, A., Marié, L., Dausse, D., Brehmer, P., Capet, X., Estrade, P., Machu, E., Ndoye, S., Grelet, J., Lazar, A., Marié, L., Dausse, D. and Brehmer, P.: On the Dynamics of the Southern Senegal Upwelling Center: Observed Variability from Synoptic to Superinertial Scales, J. Phys. Oceanogr., 47(1), 155–180, doi:10.1175/JPO-D-15-0247.1, 2017.

Cox, P. M., Pearson, D., Booth, B. B., Friedlingstein, P., Huntingford, C., Jones, C. D. and Luke, C. M.: Sensitivity of tropical carbon to climate change constrained by carbon dioxide variability, Nature, 494(7437), 341–344, doi:10.1038/nature11882, 2013.

Cropper, T. E., Hanna, E. and Bigg, G. R.: Spatial and temporal seasonal trends in coastal upwelling off Northwest Africa, 1981-2012, Deep. Res. Part I Oceanogr. Res. Pap., 86, 94–111, doi:10.1016/j.dsr.2014.01.007, 2014.

Deangelis, A. M., Qu, X., Zelinka, M. D. and Hall, A.: An observational radiative constraint on hydrologic cycle intensification, Nature, 528(7581), 249–253, doi:10.1038/nature15770, 2015.

Demarcq, H. and Faure, V.: Coastal upwelling and associated retention indices derived from satellite SST. Application to Octopus vulgaris recruitment, Oceanol. Acta, 23(4), 391–408, doi:10.1016/S0399-1784(00)01113-0, 2000.

Farikou, O., Sawadogo, S., Niang, A., Diouf, D., Brajard, J., Mejia, C., Dandonneau, Y., Gasc, G., Crepon, M. and Thiria, S.: Inferring the seasonal evolution of phytoplankton groups in the Senegalo-Mauritanian upwelling region from satellite ocean-color spectral measurements, J. Geophys. Res. Ocean., 120(9), 6581–6601, doi:10.1002/2015JC010738, 2015.

Fasullo, J. T. and Trenberth, K. E.: A less cloudy future: The role of subtropical subsidence in climate sensitivity, Science (80-.)., 338(6108), 792–794, doi:10.1126/science.1227465, 2012.

Faye, S., Lazar, A., Sow, B. A. and Gaye, A. T.: A model study of the seasonality of sea surface temperature and circulation in the Atlantic North-eastern Tropical Upwelling System, Front. Phys., 3(September), 1–20, doi:10.3389/fphy.2015.00076, 2015.

Gao, Y., Lu, J. and Leung, L. R.: Uncertainties in projecting future changes in atmospheric rivers and their impacts on heavy precipitation over Europe, J. Clim., 29(18), 6711–6726, doi:10.1175/JCLI-D-16-0088.1, 2016.

Gordon, N. D., Jonko, A. K., Forster, P. M. and Shell, K. M.: An observationally based constraint on the water-vapor feedback, J. Geophys. Res. Atmos., 118(22), 12435–12443, doi:10.1002/2013JD020184, 2013.

Hewitson, B. C. and Crane, R. G.: Self-organizing maps: Applications to synoptic climatology, Clim. Res., 22(1), 13–26, doi:10.3354/cr022013, 2002.

Huber, M. and Knutti, R.: Anthropogenic and natural warming inferred from changes in Earth's energy balance, Nat. Geosci., 5(1), 31–36, doi:10.1038/ngeo1327, 2012.

Jacox, M. G., Edwards, C. A., Hazen, E. L. and Bograd, S. J.: Coastal Upwelling Revisited: Ekman, Bakun, and Improved Upwelling Indices for the U.S. West Coast, J. Geophys. Res. Ocean., 1–19, doi:10.1029/2018JC014187, 2018.

Jain, A. K. and Dubes, R. C.: Algorithms for clustering data, Prentice Hall, Inc., Englewood. Cliffs., 1988.

Jouini, M., Lévy, M., Crépon, M. and Thiria, S.: Reconstruction of satellite chlorophyll images under heavy cloud coverage using a neural classification method, Remote Sens. Environ., 131, 232–246, doi:10.1016/j.rse.2012.11.025, 2013.

Jouini, M., Béranger, K., Arsouze, T., Beuvier, J., Thiria, S., Crépon, M. and Taupier-Letage, I.: The Sicily Channel surface circulation revisited using a neural clustering analysis of a high-resolution simulation, J. Geophys. Res. Ocean., 121(7), 4545–4567, doi:10.1002/2015JC011472, 2016.

Knutti, R., Meehl, G. A., Allen, M. R. and Stainforth, D. A.: Constraining climate sensitivity from the seasonal cycle in surface temperature, J. Clim., 19(17), 4224–4233, doi:10.1175/JCLI3865.1, 2006.

Knutti, R., Furrer, R., Tebaldi, C., Cermak, J., Meehl, G. A., Knutti, R., Furrer, R., Tebaldi, C., Cermak, J. and Meehl, G. A.: Challenges in Combining Projections from Multiple Climate Models, J. Clim., 23(10), 2739–2758, doi:10.1175/2009JCLI3361.1, 2010.

Knutti, R., Sedláček, J., Sanderson, B. M., Lorenz, R., Fischer, E. M. and Eyring, V.: A climate model projection weighting scheme accounting for performance and interdependence, Geophys. Res. Lett., 44(4), 1909–1918, doi:10.1002/2016GL072012, 2017.

Kohonen, T.: Essentials of the self-organizing map, Neural Networks, 37, 52–65, doi:10.1016/j.neunet.2012.09.018, 2013.

Kounta, L., Capet, X., Jouanno, J., Kolodziejczyk, N., Sow, B. and Gaye, A. T.: A model perspective on the dynamics of the shadow zone of the eastern tropical North Atlantic – Part 1: the poleward slope currents along West Africa, Ocean Sci., 14(5), 971–997, doi:10.5194/os-14-971-2018, 2018.

Lambert, S. M. and Boer, G. J.: CMIP1 evaluation and intercomparison of coupled climate models, Clim. Dyn., 17, 83–106, doi:10.1007/pl00013736, 2001.

Liu, Y., Weisberg, R. H. and Mooers, C. N. K.: Performance evaluation of the self-organizing map for feature extraction, J. Geophys. Res. Ocean., 111(5), C05018, doi:10.1029/2005JC003117, 2006.

Loeb, N. G., Wang, H., Cheng, A., Kato, S., Fasullo, J. T., Xu, K.-M. and Allan, R. P.:

Observational constraints on atmospheric and oceanic cross-equatorial heat transports: revisiting the precipitation asymmetry problem in climate models, Clim. Dyn., 46(9–10), 3239–3257, doi:10.1007/s00382-015-2766-z, 2015.

Lutz, A. F., ter Maat, H. W., Biemans, H., Shrestha, A. B., Wester, P. and Immerzeel, W. W.: Selecting representative climate models for climate change impact studies: an advanced envelope-based selection approach, Int. J. Climatol., 36(12), 3988–4005, doi:10.1002/joc.4608, 2016.

Masson, D. and Knutti, R.: Climate model genealogy, Geophys. Res. Lett., 38(8), doi:10.1029/2011GL046864, 2011.

Monteleoni, C., Schmidt, G. A., Alexander, F., Niculescu-Mizil, A., Steinhaeuser, K., Tippett, M., Banerjee, A., Benno Blumenthal, M., Ganguly, A. R., Smerdon, J. E. and Tedesco, M.: Climate informatics, in Computational Intelligent Data Analysis for Sustainable Development, pp. 81–126, NASA., 2016.

Ndoye, S., Capet, X., Estrade, P., Sow, B. A., Dagorne, D., Lazar, A., Gaye, A. T. and Brehmer, P.: SST patterns and dynamics of the southern Senegal-Gambia upwelling center, J. Geophys. Res. Ocean., 119(12), 8315–8335, doi:10.1002/2014JC010242, 2014.

Niang, A., Gross, L., Thiria, S., Badran, F. and Moulin, C.: Automatic neural classification of ocean colour reflectance spectra at the top of the atmosphere with introduction of expert knowledge, Remote Sens. Environ., 86(2), 257–271, doi:10.1016/S0034-4257(03)00113-5, 2003.

Niang, A., Badran, F., Moulin, C., Crépon, M. and Thiria, S.: Retrieval of aerosol type and optical thickness over the Mediterranean from SeaWiFS images using an automatic neural classification method, Remote Sens. Environ., 100(1), 82–94, doi:10.1016/j.rse.2005.10.005, 2006.

O'Gorman, P. A., Allan, R. P., Byrne, M. P. and Previdi, M.: Energetic Constraints on Precipitation Under Climate Change, Surv. Geophys., 33(3–4), 585–608, doi:10.1007/s10712-011-9159-6, 2012.

Phillips, T. J. and Gleckler, P. J.: Evaluation of continental precipitation in 20th century climate simulations: The utility of multimodel statistics, Water Resour. Res., 42(3), doi:10.1029/2005WR004313, 2006.

Praveen Kumar, B., Vialard, J., Lengaigne, M., Murty, V. S. N. and McPhaden, M. J.: TropFlux: air-sea fluxes for the global tropical oceans—description and evaluation, Clim. Dyn., 38(7–8), 1521–1543, doi:10.1007/s00382-011-1115-0, 2011.

Rayner, N. A.: Global analyses of sea surface temperature, sea ice, and night marine air temperature since the late nineteenth century, J. Geophys. Res., 108(D14), 4407, doi:10.1029/2002JD002670, 2003.

Reichler, T. and Kim, J.: How well do coupled models simulate today's climate?, Bull. Am. Meteorol. Soc., 89(3), 303–311, doi:10.1175/BAMS-89-3-303, 2008.

Reifen, C. and Toumi, R.: Climate projections: Past performance no guarantee of future skill?, Geophys. Res. Lett., 36(13), 1–5, doi:10.1029/2009GL038082, 2009.

Reusch, D. B., Alley, R. B. and Hewitson, B. C.: North Atlantic climate variability from a self-organizing map perspective, J. Geophys. Res. Atmos., 112(2), D02104, doi:10.1029/2006JD007460, 2007.

Richardson, A. J., Risi En, C. and Shillington, F. A.: Using self-organizing maps to identify patterns in satellite imagery, Prog. Oceanogr., 59(2–3), 223–239, doi:10.1016/j.pocean.2003.07.006, 2003.

Rykaczewski, R. R., Dunne, J. P., Sydeman, W. J., García-Reyes, M., Black, B. A. and Bograd,

S. J.: Poleward displacement of coastal upwelling-favorable winds in the ocean's eastern boundary currents through the 21st century, Geophys. Res. Lett., 42(15), 6424–6431, doi:10.1002/2015GL064694, 2015.

Santer, B. D., Taylor, K. E., Gleckler, P. J., Bonfils, C., Barnett, T. P., Pierce, D. W., Wigley, T. M. L., Mears, C., Wentz, F. J., Bruggemann, W., Gillett, N. P., Klein, S. A., Solomon, S., Stott, P. A. and Wehner, M. F.: Incorporating model quality information in climate change detection and attribution studies, Proc. Natl. Acad. Sci., 106(35), 14778–14783, doi:10.1073/pnas.0901736106, 2009.

Sawadogo, S., Brajard, J., Niang, A., Lathuiliere, C., Crépon, M. and Thiria, S.: Analysis of the Senegalo-Mauritanian upwelling by processing satellite remote sensing observations with topological maps., in Proceedings of the International Joint Conference on Neural Networks, pp. 2826–2832, IEEE., 2009.

Sirven, J., Mignot, J. and Crépon, M.: Generation of Rossby waves off the Cape Verde Peninsula: The role of the coastline, Ocean Sci., 15(6), 1667–1690, doi:10.5194/os-15-1667-2019, 2019.

Smith, T. M., Reynolds, R. W., Peterson, T. C. and Lawrimore, J.: Improvements to NOAA's historical merged land-ocean surface temperature analysis (1880-2006), J. Clim., 21(10), 2283–2296, doi:10.1175/2007JCLI2100.1, 2008.

Son, S. W., Gerber, E. P., Perlwitz, J., Polvani, L. M., Gillett, N. P., Seo, K. H., Eyring, V., Shepherd, T. G., Waugh, D., Akiyoshi, H., Austin, J., Baumgaertner, A., Bekki, S., Braesicke, P., Brühl, C., Butchart, N., Chipperfield, M. P., Cugnet, D., Dameris, M., Dhomse, S., Frith, S., Garny, H., Garcia, R., Hardiman, S. C., Jöckel, P., Lamarque, J. F., Mancini, E., Marchand, M., Michou, M., Nakamura, T., Morgenstern, O., Pitari, G., Plummer, D. A., Pyle, J., Rozanov, E., Scinocca, J. F., Shibata, K., Smale, D., Teyssdre, H., Tian, W. and Yamashita, Y.: Impact of stratospheric ozone on Southern Hemisphere circulation change: A multimodel assessment, J. Geophys. Res. Atmos., 115(19), D00M07, doi:10.1029/2010JD014271, 2010.

Stegehuis, A. I., Vautard, R., Ciais, P., Teuling, A. J., Jung, M. and Yiou, P.: Summer temperatures in Europe and land heat fluxes in observation-based data and regional climate model simulations, Clim. Dyn., 41(2), 455–477, doi:10.1007/s00382-012-1559-x, 2013.

Stocker, T. F., Qin, D., Plattner, G.-K., Tignor, M., Allen, S. K., Boschung, J., Nauels, A., Xia, Y., Bex, V. and Midgley, P. M., Eds.: Climate Change 2013: The Physical Science Basis. Contribution of Working Group I to the Fifth Assessment Report of the Intergovernmental Panel on Climate Change, Cambridge University Press, United Kingdom and New York, NY, USA., 2013.

Sylla, A., Mignot, J., Capet, X. and Gaye, A. T.: Weakening of the Senegalo–Mauritanian upwelling system under climate change, Clim. Dyn., 53(7), 4447–4473, doi:10.1007/s00382-019-04797-y, 2019.

Tan, I., Storelvmo, T. and Zelinka, M. D.: Observational constraints on mixed-phase clouds imply higher climate sensitivity, Science (80-.)., 352(6282), 224–227, doi:10.1126/science.aad5300, 2016.

Taylor, K. E., Stouffer, R. J., Meehl, G. A., Taylor, K. E., Stouffer, R. J. and Meehl, G. A.: An Overview of CMIP5 and the Experiment Design, Bull. Am. Meteorol. Soc., 93(4), 485–498, doi:10.1175/BAMS-D-11-00094.1, 2012.

Tebaldi, C. and Knutti, R.: The use of the multi-model ensemble in probabilistic climate projections, Philos. Trans. R. Soc. A Math. Phys. Eng. Sci., 365(1857), 2053–2075, doi:10.1098/rsta.2007.2076, 2007.

Wang, D., Gouhier, T. C., Menge, B. A. and Ganguly, A. R.: Intensification and spatial homogenization of coastal upwelling under climate change, Nature, 518(7539), 390–394, doi:10.1038/nature14235, 2015.

Wenzel, S., Cox, P. M., Eyring, V. and Friedlingstein, P.: Emergent constraints on climate-carbon cycle feedbacks in the CMIP5 Earth system models, J. Geophys. Res. Biogeosciences, 119(5), 794–807, doi:10.1002/2013JG002591, 2014.

Wenzel, S., Eyring, V., Gerber, E. P. and Karpechko, A. Y.: Constraining future summer austral jet stream positions in the CMIP5 ensemble by process-oriented multiple diagnostic regression, J. Clim., 29(2), 673–687, doi:10.1175/JCLI-D-15-0412.1, 2016.

1

2 **APPENDIX**

3

Model-group 1	Model-group 2	Model-group 3	Model-group 4
ACCESS1-0	bcc-csm1-1	FGOALS-g2	CanCM4
ACCESS1-3	bcc-csm1-1-m	GISS-E2-H	CanESM2
CESM1-CAM5	BNU-ESM	GISS-E2-H-CC	CMCC-CESM
CESM1-CAM5-1-FV2	CCSM4	GISS-E2-R	CMCC-CM
CESM1-WACCM	CESM1-BGC	GISS-E2-R-CC	**CMCC-CMS**
HadCM3	CESM1-FASTCHEM	inmcm4	**CNRM-CM5**
MIROC-ESM	GFDL-CM2p1	IPSL-CM5A-LR	**CNRM-CM5-2**
MIROC-ESM-CHEM	GFDL-ESM2G	IPSL-CM5A-MR	CSIRO-Mk3-6-0
MIROC5	GFDL-ESM2M	IPSL-CM5B-LR	**FGOALS-s2**
NorESM1-M	MPI-ESM-LR	MRI-CGCM3	**GFDL-CM3**
NorESM1-ME	MPI-ESM-MR	MRI-ESM1	HadGEM2-AO
	MPI-ESM-P		HadGEM2-CC
			HadGEM2-ES

4

ZModel-group 1	ZModel-group 2	ZModel-group 3	ZModel-group 4
ACCESS1-0	**CMCC-CMS**	BNU-ESM	ACCESS1-3
bcc-csm1-1-m	**CNRM-CM5**	CanCM4	bcc-csm1-1
CCSM4	**CNRM-CM5-2**	CanESM2	CSIRO-Mk3-6-0
CESM1-BGC	**FGOALS-s2**	CMCC-CM	HadGEM2-AO
CESM1-CAM5	**GFDL-CM3**	FGOALS-g2	HadGEM2-CC
CESM1-CAM5-1-FV2		IPSL-CM5A-LR	HadGEM2-ES
CESM1-FASTCHEM		IPSL-CM5A-MR	MIROC-ESM
CESM1-WACCM		MRI-CGCM3	MIROC-ESM-CHEM
GISS-E2-H		NorESM1-M	MRI-ESM1
GISS-E2-H-CC		NorESM1-ME	
GISS-E2-R			
GISS-E2-R-CC			**ZModel-group 5**
HadCM3			
inmcm4			CMCC-CESM
IPSL-CM5B-LR			GFDL-CM2p1
MIROC5			GFDL-ESM2G
MPI-ESM-LR			GFDL-ESM2M
MPI-ESM-MR			
MPI-ESM-P			

5

6 Table A1: Composition of the different Model-groups identified in the main text. In bold, we

7 show the CMIP5 models which belong to Model-group 4 and ZModel-group 2. We note that all

8 the models belonging to Zmodel-group 2 also belong to Model-group 4.

9

nb	Model Acronym	nb	Model Acronym
1	bcc-csm1-1	25	HadGEM2-ES
2	bcc-csm1-1-m	26	MPI-ESM-LR
3	BNU-ESM	27	MPI-ESM-MR
4	CanCM4	28	MPI-ESM-P
5	CanESM2	29	MRI-CGCM3
6	CMCC-CESM	30	MRI-ESM1
7	CMCC-CM	31	GISS-E2-H
8	CMCC-CMS	32	GISS-E2-H-CC
9	CNRM-CM5	33	GISS-E2-R
10	CNRM-CM5-2	34	GISS-E2-R-CC
11	ACCESS1-0	35	CCSM4
12	ACCESS1-3	36	NorESM1-M
13	CSIRO-Mk3-6-0	37	NorESM1-ME
14	inmcm4	38	HadGEM2-AO
15	IPSL-CM5A-LR	39	GFDL-CM2p1
16	IPSL-CM5A-MR	40	GFDL-CM3
17	IPSL-CM5B-LR	41	GFDL-ESM2G
18	FGOALS-g2	42	GFDL-ESM2M
19	FGOALS-s2	43	CESM1-BGC
20	MIROC-ESM	44	CESM1-CAM5
21	MIROC-ESM-CHEM	45	CESM1-CAM5-1-FV2
22	MIROC5	46	CESM1-FASTCHEM
23	HadCM3	47	CESM1-WACCM
24	HadGEM2-CC		

Table 1: List of the CMIP5 models used for the comparison. The reader is referred to the CMIP5 documentation for more information on each of them. Here, each configuration is furthermore given a number, for easier identification in subsequent figures.

1
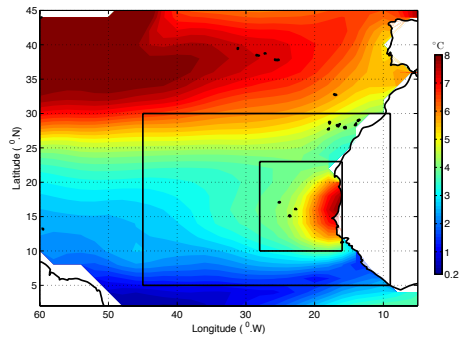
2

3 Figure 1: Amplitude of the SST seasonal anomalies in the western tropical north Atlantic. SST
4 data are from the ERSSTv3b data set averaged between 1975 and 2005. The two black boxes
5 show the extended and zoomed regions respectively, over which the statistical classifications
6 were performed (see text for details).
7
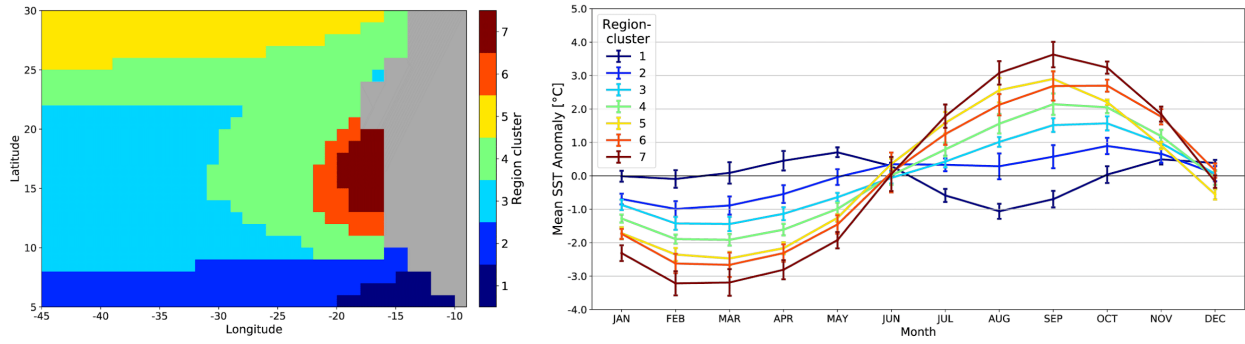
Figure 2: Left panel: Region-clusters associated with the SOM-clusters obtained after a HAC on a 30x4 neuron SOM learned on ERSSTv3b observations in the extended zone (see text for details). Right Panel: Ensemble-mean climatological SST anomalies for the grid points of the seven Region-clusters. The error bars show the standard deviation of this ensemble mean.
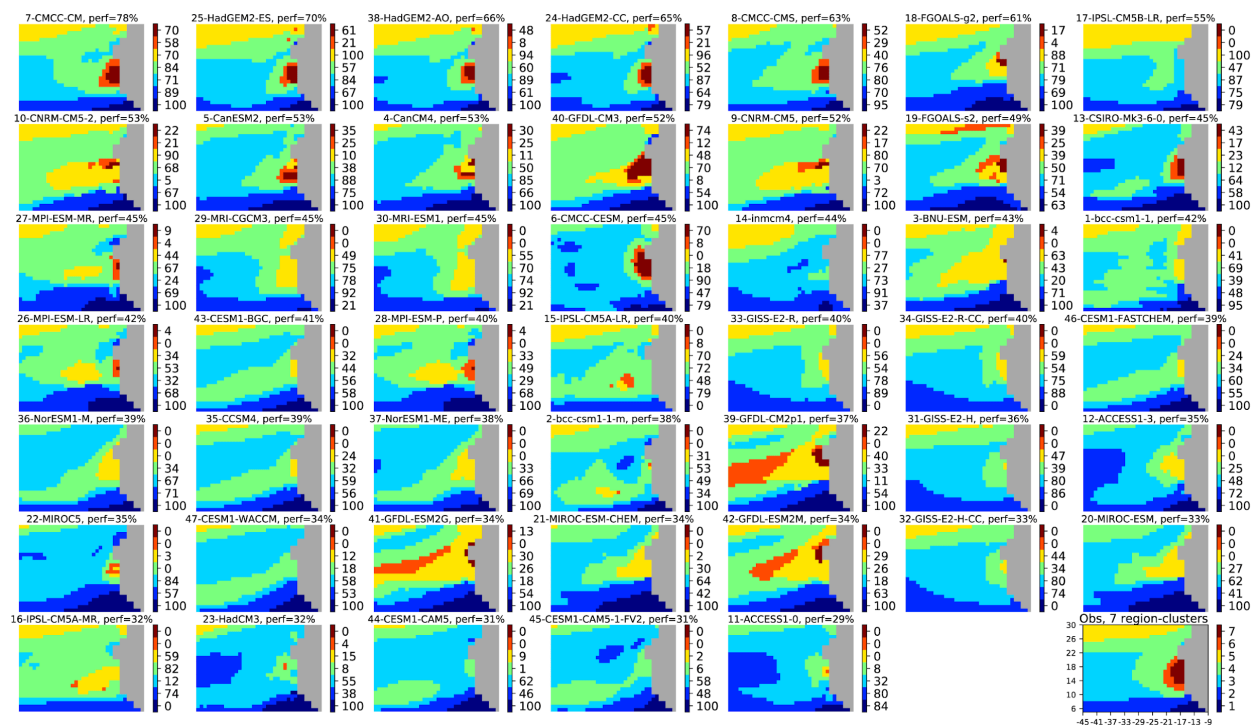
Figure 3: Projection of the 47 climate models of the CMIP5 database onto the SOM learned with ERSSTv3b climatology in the extended zone (see Fig. 1). On top of each panel, we figure: the number referencing the model, its name (Table 1), and its skill given as a mean percentage (see text). The models are ordered according to their skill in decreasing order. The 7 Region-clusters (or SOM-clusters) are defined by applying an HAC to the SOM output learned with the observation field. They are represented by different colors. The numbers in the colorbar at the right of each panel represent the skill for each Region-cluster. The observation field is shown in the bottom right panel and the numbers in front of the colorbar reference the Region-cluster.
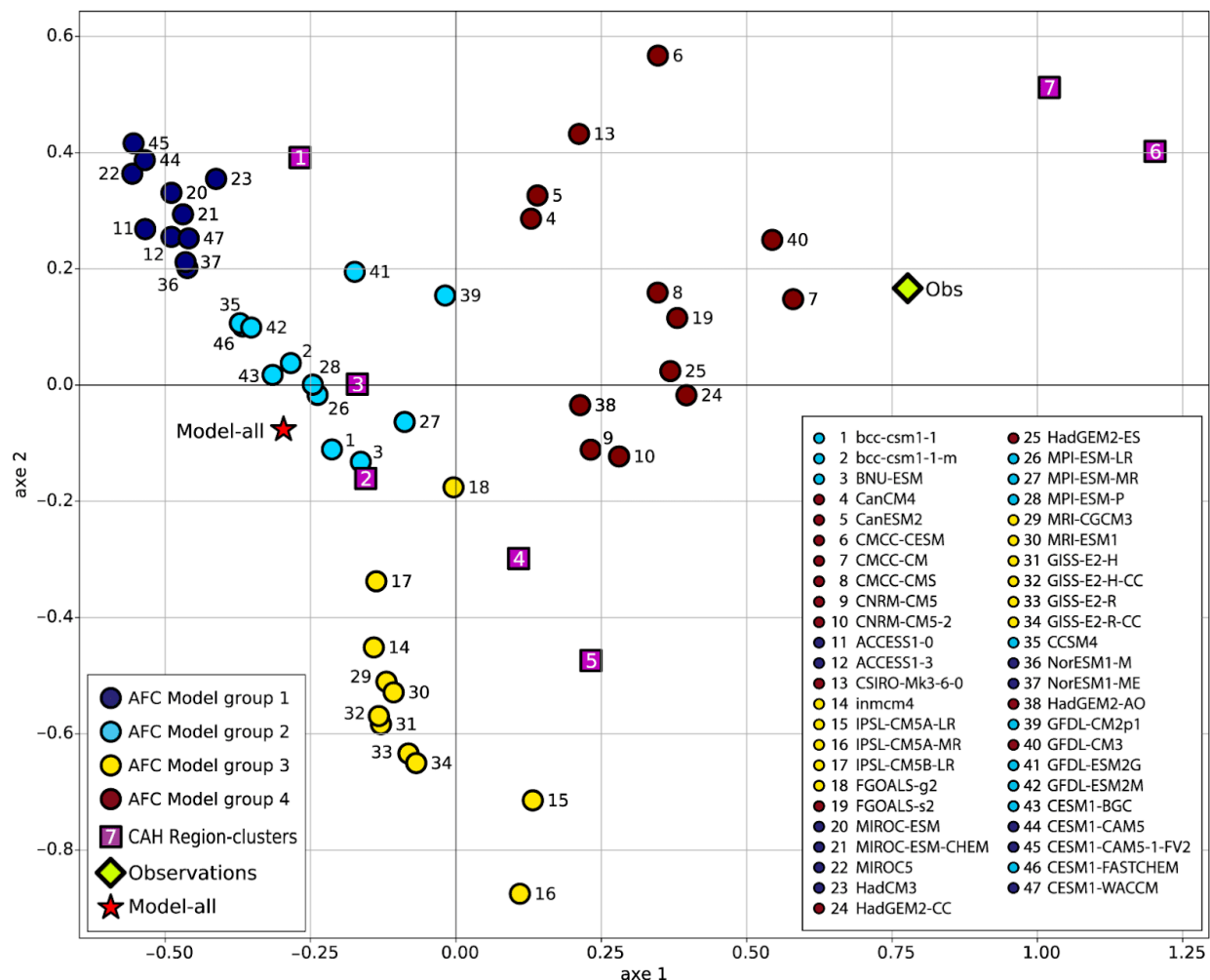
Figure 4: Projection of the CMIP5 models (colored circles) and the observation field (green diamond) defined by their cluster skill vectors on the first two axis of the MCA. The seven region-clusters of the observation field are represented by purple squares. The colours of the circles denote the four groups of models obtained after an HAC was performed on the seven MCA components of the models. The projection of the full multi-model mean (47 models) is represented by a red star. We stress here the fact that representing the full MCA output is complicated because of the multidimensional property. The representation of some data along the first two axis as here can be biased because of the importance of the other axes.
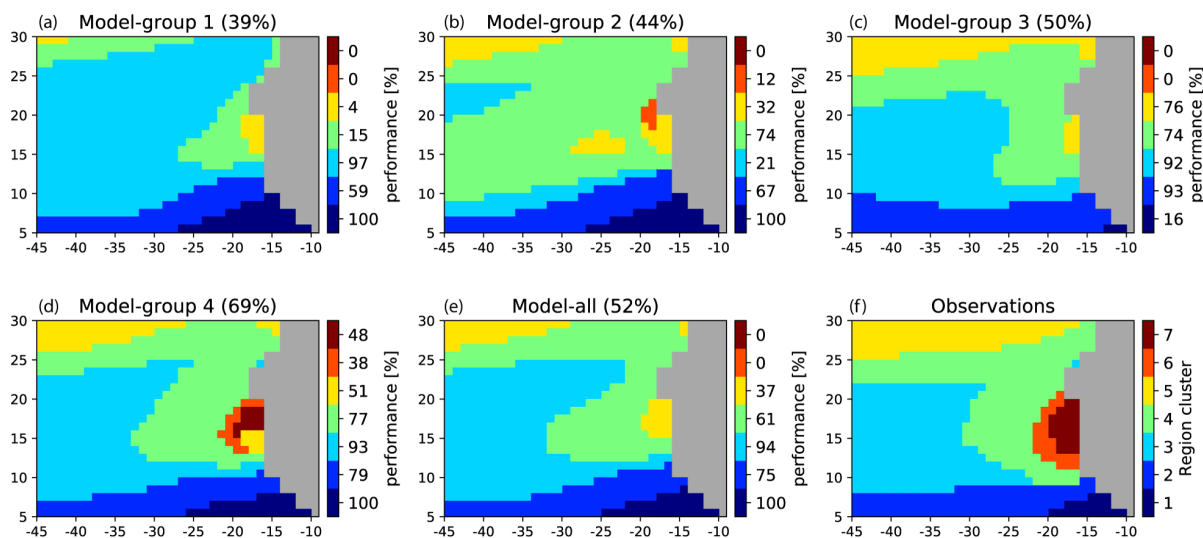
Figure 5: (a)-(d): Projection of the multi-model ensembles (Model-group) onto the SOM learned with ERSSTv3b climatology in the extended zone. Multi-model ensemble performances are obtained by averaging the skill of the models forming each group. The performances are given on top of each panel. The Region-clusters determined by processing the observations in the extended area and their associated colors are given in the bottom right panel. The colorbars at the right of each multi-ensemble panel represent the skill (in %) associated with each Region-cluster. Panel (e) shows the same for the full multi-model ensemble. Panel (f) reproduces the Region-clusters based on the observations also shown in Fig. 2.
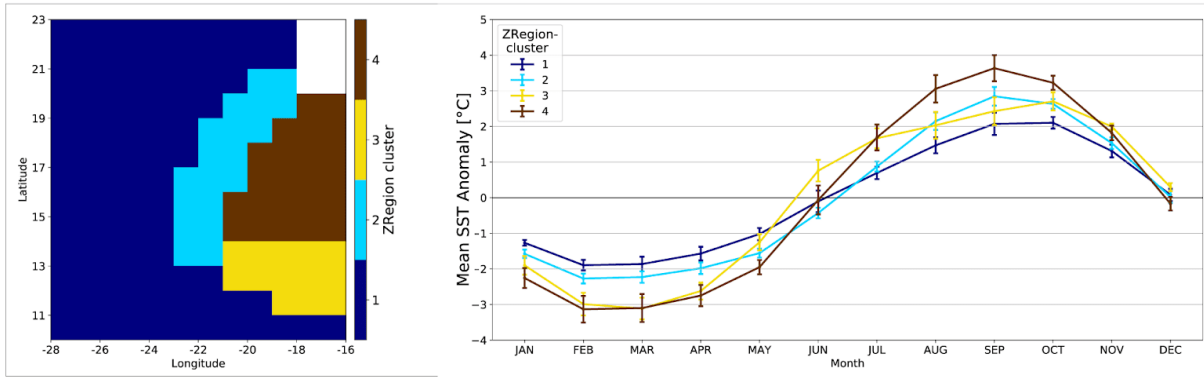
Figure 6: Left panel: ZRegion-clusters associated with the ZSOM-clusters obtained after a HAC on a 10x12 neuron SOM learned on ERSSTv3b observations in the zoomed zone (see text for details). Right Panel: Ensemble-mean climatological SST anomalies for the grid points of the four ZRegion-clusters. The error bars show the standard deviation of this ensemble mean.
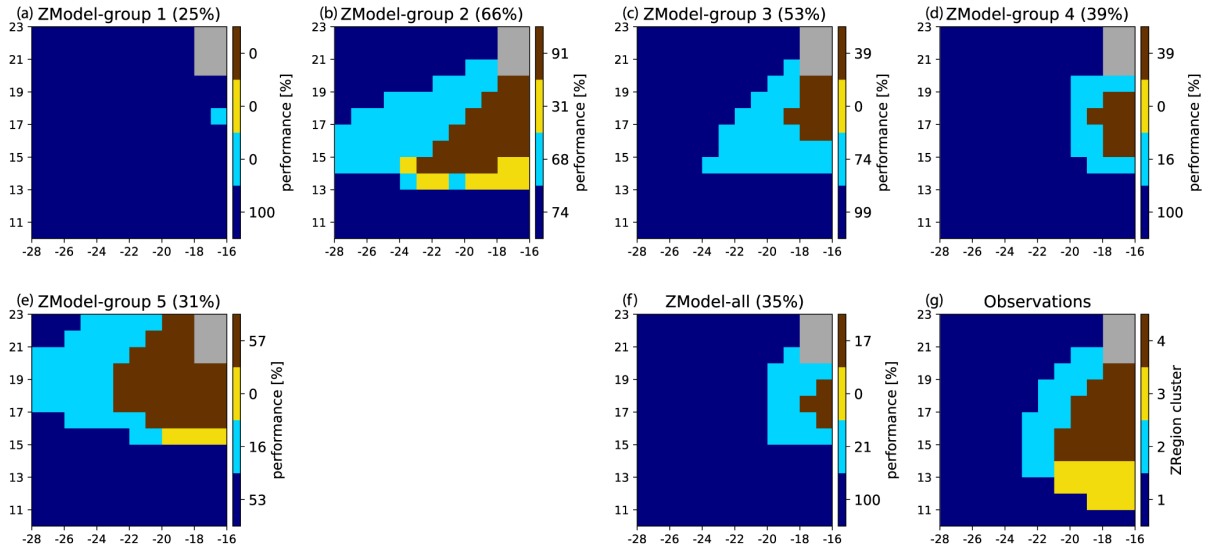
Figure 7: (a)-(e): Projection of the multi-model ensembles (ZModel-groups) onto the ZSOM. The performances are given on top of each panel. The ZRegion-clusters determined by processing the observations in the zoomed region and their associated colors are given in the bottom right panel. The colorbars at the right of each multi-ensemble panel represent the skill (in %) associated with each ZRegion-cluster. Panel (f) shows the same for the full multi-model ensemble. Panel (g) reproduces the Region-clusters based on the observations also shown in Fig. 6.
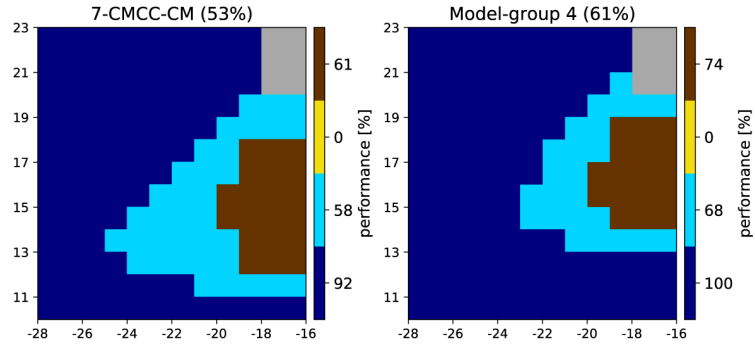
Figure 8 : Same as Fig. 7 but for the individual model CMCC-CM (model 7) (left) and the Model-group 4 (right).
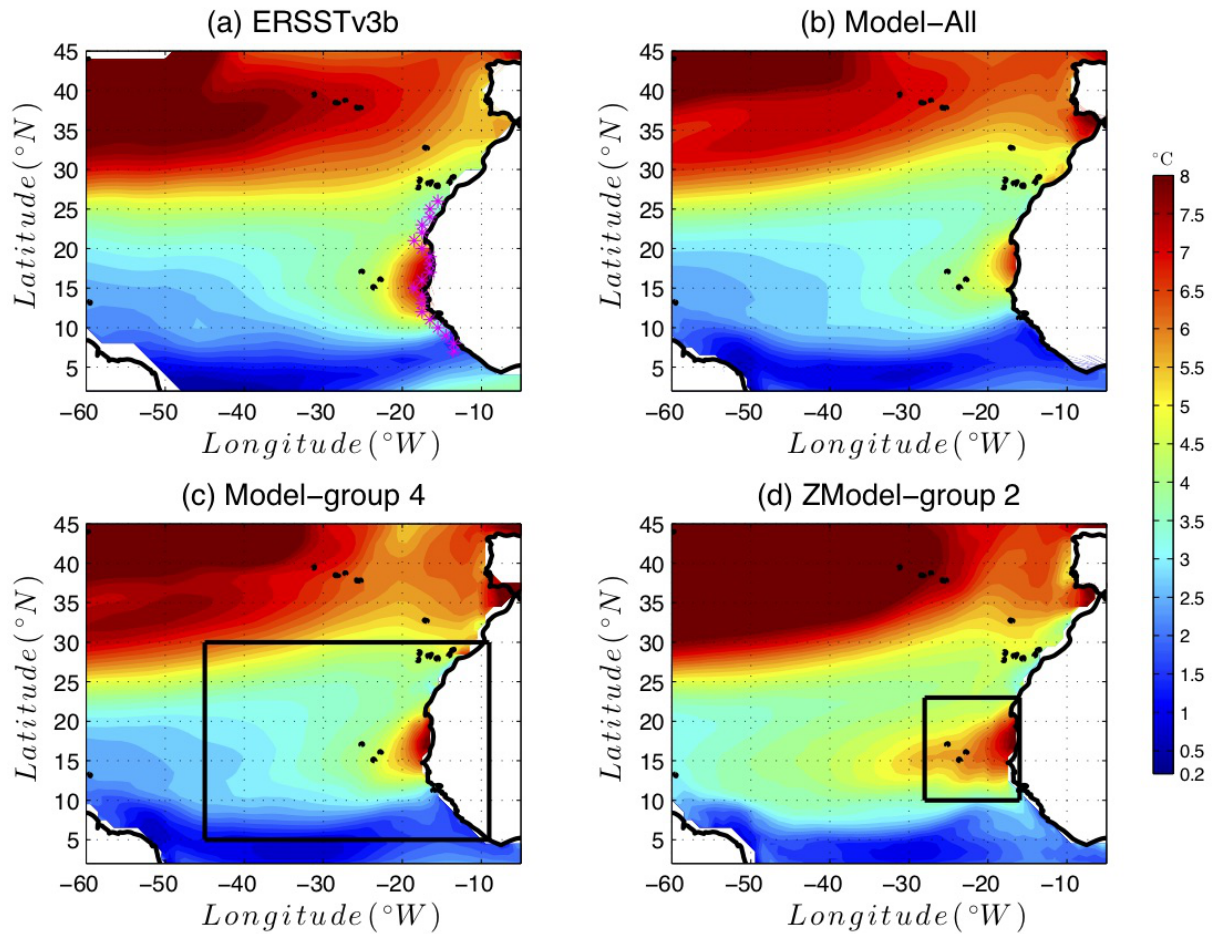
Figure 9: Amplitude of the SST seasonal cycle in the (a) ERSSTv3b Observations (b) Model-All, c) Model-group 4 (best Model-group for the extended area, figured out by the black rectangular box) and (d) ZModel-group 2 (best Model-group for the reduced area, figured out by the small black rectangular box). The SST seasonal cycle is computed over the period 1985-2005
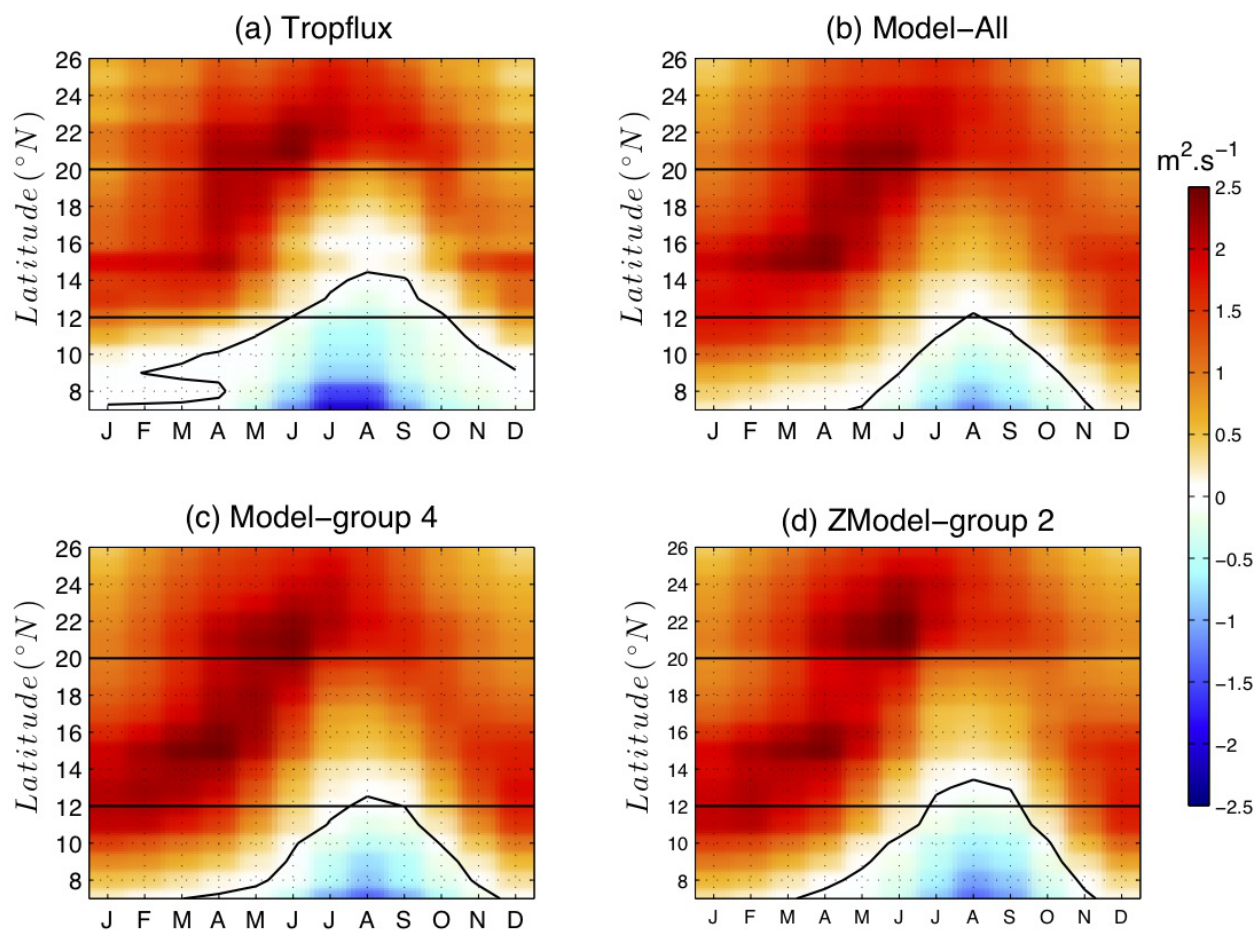
Figure 10: Latitude-time plot of depth integrated Ekman transport computed over the grid point located along the coast (magenta stars in Fig. 9.a). The time axis shows climatological months over the period 1985-2005. Positive (negative) values correspond to upwelling (downwelling) conditions. Panel (a) stands for TropFlux data set (see (Praveen Kumar et al., 2011) (b) Model-All, (c) Model-group 4 and (d) ZModel-group 2. In each panel, the black contour shows the contour zero. The horizontal dashed lines are positioned at 12°N and 20°N and give a rough limitation of the senegalo-mauritanian upwelling region.
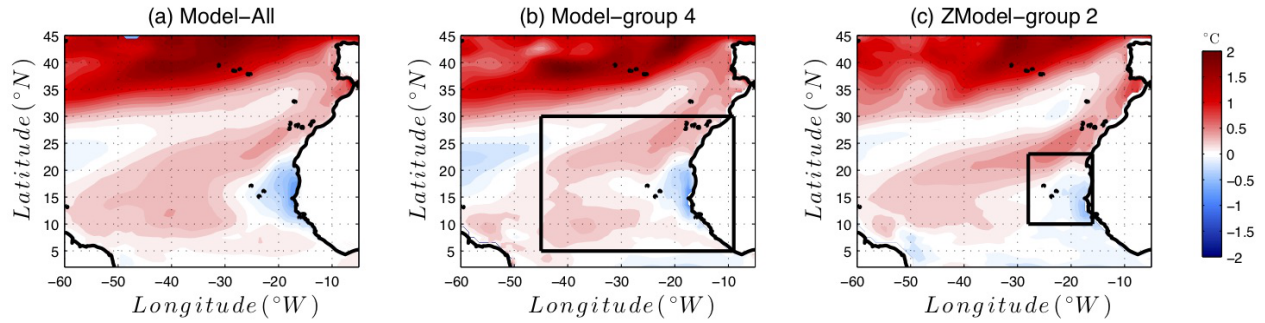
Figure 11: Evolution of the amplitude of the SST seasonal cycle at the end of the 21st century. The figure shows the difference between the seasonal cycle amplitude averaged over the period [2080-2100] following the RCP8.5 scenario and the amplitude averaged over the period [1985-2005] in the historical simulations. A positive value (red) means that the seasonal cycle is more marked over the period 2080-2100.
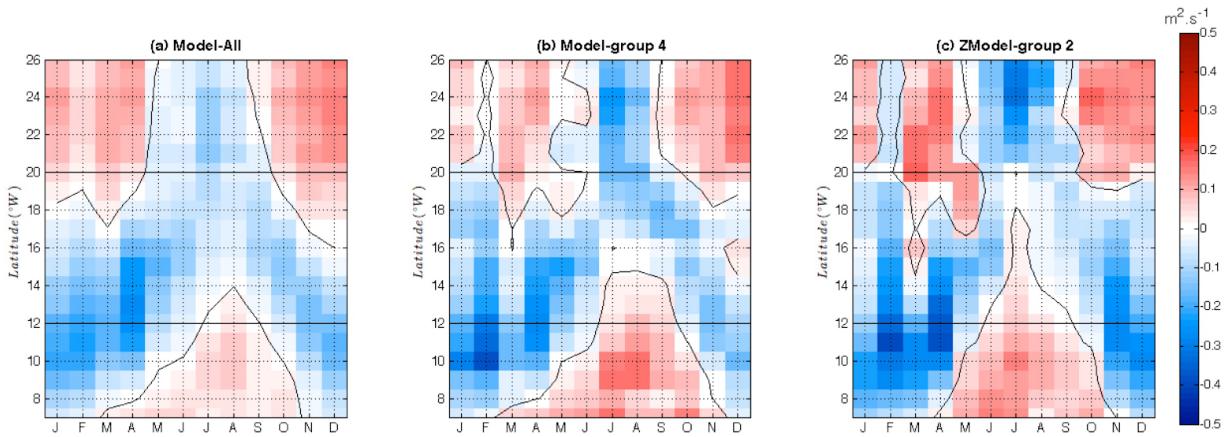
Figure 12: Latitude-time diagram of the seasonal shift of the meridional component of the wind-stress with respect to the present days. For each month and at each latitude, we show the meridional wind stress shift with respect to the present days averaged over the period [2080-2100]. Positive values (red) means that the wind stress shift is southward and is thus favorable to upwelling. Panel (a) stands for Model-All, (b) Model-group 4 and (c) ZModel-group 2.